18. T. Alerstam, D. Christie, A. Ulfstrand, *Bird Migration* (Cambridge Univ. Press, 1993).
19. F. Liechti, W. Witvliet, R. Weber, E. Bächler, *Nat. Commun.* **4**, 2554 (2013).
20. N. C. Rattenborg, *Naturwissenschaften* **93**, 413–425 (2006).
21. J. A. Lesku *et al*., *Science* **337**, 1654–1658 (2012).
22. H. Weimerskirch, M. Louzao, S. de Grissac, K. Delord, *Science* **335**, 211–214 (2012).
23. U. C. Mohanty, M. Mohapatra, O. P. Singh, B. K. Bandyopadhyay, L. S. Rathore, *Monitoring and Prediction of Tropical Cyclones in the Indian Ocean and Climate Change* (Springer, Dordrecht, Netherlands, 2014).
24. H. J. J. Jonker, T. Heus, P. P. Sullivan, *Geophys. Res. Lett.* **35**, L07810 (2008).

ACKNOWLEDGMENTS

The tracking data presented in the paper are available from the Dryad Digital Repository. We thank the Forces Armées de la Zone Sud de l'Océan Indien for transport and logistical support on Europa Island and the TAAF Administration for allowing us to work on Europa Island. We thank the fieldworkers involved in the study on Europa, in particular J. B. Pons and R. Weimerskirch; R. Spivey for help with preparing the electrocardiogram and acceleration tags and for the data processing of the heart rate recording; and A. Corbeau for help with data analyses. The study is a contribution to the Program EARLYLIFE funded by a European Research Council Advanced Grant under the European Community's Seven Framework Program FP7/2007–2013 (grant agreement ERC-2012-ADG_20120314 to H.W.). We thank Y. Ropert-Coudert, Y. Cherel, and two anonymous reviewers for helpful comments on earlier versions of the manuscript.

SUPPLEMENTARY MATERIALS

www.sciencemag.org/content/353/6294/74/suppl/DC1
Materials and Methods
Supplementary Text
Figs. S1 to S10
Table S1
References (*25*–*34*)

11 February 2016; accepted 20 May 2016
10.1126/science.aaf4374

TRANSCRIPTION

Visualization and analysis of gene expression in tissue sections by spatial transcriptomics

Patrik L. Ståhl,[1,2]* Fredrik Salmén,[2]* Sanja Vickovic,[2]† Anna Lundmark,[2,3]† José Fernández Navarro,[1,2] Jens Magnusson,[1] Stefania Giacomello,[2] Michaela Asp,[2] Jakub O. Westholm,[4] Mikael Huss,[4] Annelie Mollbrink,[2] Sten Linnarsson,[5] Simone Codeluppi,[5,6] Åke Borg,[7] Fredrik Pontén,[8] Paul Igor Costea,[2] Pelin Sahlén,[2] Jan Mulder,[9] Olaf Bergmann,[1] Joakim Lundeberg,[2]‡ Jonas Frisén[1]

Analysis of the pattern of proteins or messenger RNAs (mRNAs) in histological tissue sections is a cornerstone in biomedical research and diagnostics. This typically involves the visualization of a few proteins or expressed genes at a time. We have devised a strategy, which we call "spatial transcriptomics," that allows visualization and quantitative analysis of the transcriptome with spatial resolution in individual tissue sections. By positioning histological sections on arrayed reverse transcription primers with unique positional barcodes, we demonstrate high-quality RNA-sequencing data with maintained two-dimensional positional information from the mouse brain and human breast cancer. Spatial transcriptomics provides quantitative gene expression data and visualization of the distribution of mRNAs within tissue sections and enables novel types of bioinformatics analyses, valuable in research and diagnostics.

Tissue transcriptomes are typically studied by RNA-sequencing (RNA-seq) (*1*) of homogenized biopsies, which results in an averaged transcriptome and loss of spatial information. The positional context of gene expression is of key importance to understanding tissue functionality and pathological changes. Several strategies have recently been developed with this aim (*2*–*5*), but they have limitations in the number of transcripts that can be analyzed, rely on rich preexisting data sets, and/or are costly and labor-intensive, and none of them are operational in the standard research and diagnostic setting of regular histological tissue sections.

We asked whether it would be possible to introduce positional molecular barcodes in the complementary DNA (cDNA) synthesis reaction within the context of an intact tissue section before RNA-seq. We first assessed whether it was feasible to generate cDNA from messenger RNA (mRNA) in tissue sections on a surface. We immobilized reverse-transcription oligo(dT) primers on glass slides and placed on the slides sections of adult mouse olfactory bulb, a brain region with clear histological landmarks and ample gene-expression reference data. The tissue was fixed, stained, and imaged (Fig. 1A) (*6*).

After permeabilization, we added reverse-transcription reagents on top of the tissue. We used fluorescently labeled nucleotides to visualize the synthesized cDNA (Fig. 1A and fig. S1). The tissue was then enzymatically removed, which left cDNA coupled to the arrayed oligonucleotides on the slide (*6*). The fluorescent cDNA showed a pattern in detail corresponding to the tissue structure revealed by the general histology (Fig. 1, B and C), and the cDNA was strictly localized directly under individual cells (Fig. 1, D to G′). By comparing the hematoxylin-and-eosin and fluorescent signals, we could measure the average distance of diffusion outside the border of a cell to 1.7 ± 2 μm (mean ± SD) (fig. S1, E to H).

The realization that it is possible to capture mRNA in tissue sections with minimal diffusion and maintained positional representation motivated us to array oligonucleotides with positional barcodes (Fig. 2A), and we denoted this strategy "spatial transcriptomics." We deposited ~200 million oligonucleotides in each of 1007 features, with a diameter of 100 μm and a center-to-center distance of 200 μm, over an area of 6.2 mm by 6.6 mm (fig. S2).

After capturing and reverse-transcribing mRNA, we generated sequencing libraries based on amplification by in vitro transcription (fig. S3, A and B) (*7*, *8*). Comparison with data from RNA extracted and fragmented in solution revealed that ~95% of the genes found with one of the methods was also found with the other (fig. S3C). The correlation between the surface and in-solution libraries was $r = 0.94$, with even representation of genes having high or low expression (fig. S3D). Replicates of surface-based experiments of adjacent tissue sections showed a correlation of $r = 0.97$ (fig. S3E). Thus, cDNA synthesis from tissue with arrayed oligonucleotides on a surface is efficient and does not introduce bias compared with in-solution protocols (fig. S3F and table S1).

We sorted the RNA-seq data to its corresponding array features by using the spatial barcodes and aligned the tissue image with the features of the array, which enabled visualization and analyses. Examples of gene-expression patterns revealed by spatial transcriptomics and validation by in situ hybridization are shown in Fig. 2B and fig. S4, A to C. Transcripts expressed at very low levels, such as olfactory receptor mRNAs (*9*), were also detected with spatial transcriptomics (fig. S4D).

The number of genes (*10*) (Fig. 2C) and unique transcripts (fig. S5A) per individual feature varied between cell layers with different cell density (Fig. 2D and table S2). For the vast majority of genes, the coefficient of variation decreased as the average expression increased (fig. S5B). The number of

[1]Department of Cell and Molecular Biology, Karolinska Institute, SE-171 77 Stockholm, Sweden. [2]Science for Life Laboratory, Division of Gene Technology, KTH Royal Institute of Technology, SE-106 91 Stockholm, Sweden. [3]Department of Dental Medicine, Division of Periodontology, Karolinska Institute, SE-141 04 Huddinge, Sweden. [4]Science for Life Laboratory, Department of Biochemistry and Biophysics, Stockholm University, Box 1031, SE-171 21 Solna, Sweden. [5]Division of Molecular Neuroscience, Department of Medical Biochemistry and Biophysics, Karolinska Institute, SE-17177 Stockholm, Sweden. [6]Department of Physiology and Pharmacology, Karolinska Institute, SE-17177 Stockholm, Sweden. [7]Division of Oncology and Pathology, Department of Clinical Sciences Lund, Lund University, SE-223 81 Lund, Sweden. [8]Department of Immunology, Genetics and Pathology, Uppsala University, SE-751 85 Uppsala, Sweden. [9]Science for Life Laboratory, Department of Neuroscience, Karolinska Institute, SE-171 77 Stockholm, Sweden.
*These authors contributed equally to this work. †These authors contributed equally to this work. ‡Corresponding author. Email: joakim.lundeberg@scilifelab.se

10x Genomics EX1016

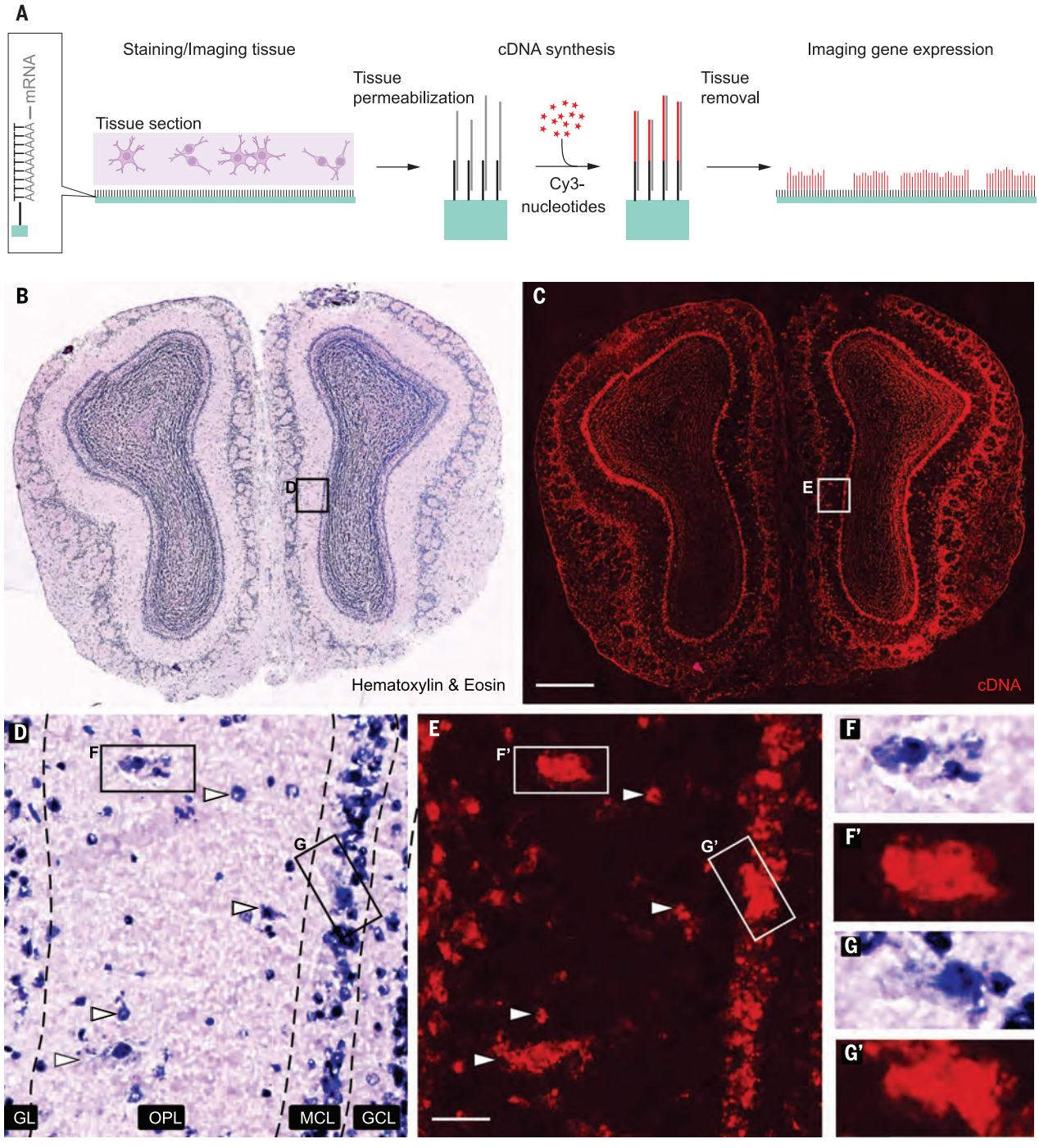


Fig. 1. Spatially localized cDNA synthesis. (**A**) The tissue is sectioned, placed onto oligo(dT) primers, stained, and imaged. cDNA synthesis with Cy3-labeled nucleotides reveals fluorescent cDNA after tissue removal. (**B**) Hematoxylin-and-eosin staining of olfactory bulbs and (**C**) fluorescent cDNA after tissue removal. Scale bar, 500 μm. (**D** and **E**) Magnification of boxes in (B) and (C). Cell layers: GL; OPL, outer plexiform layer; MCL; and GCL. Arrowheads and boxes indicate individual cells and corresponding cDNA with overlapping positions. Scale bar, 40 μm. (**F** to **G'**) Cells in (D) and (E) magnified showing cytoplasm and corresponding cDNA.

genes and transcripts captured was at least twice as high as when using laser capture microdissection (*11*), and spatial transcriptomics detected almost twice as many genes as examination by in situ hybridization in the Allen Brain Atlas (fig. S5, C and D). Furthermore, we compared spatial transcriptomics with the near-100% sensitivity of single-molecule fluorescent in situ hybridization in adjacent tissue sections. The sensitivity of spatial transcriptomics was 6.9 ± 1.5% of single-molecule fluorescent in situ hybridization (fig. S6). By comparison, single-cell RNA sequencing has been reported to have about 5 to 40% sensitivity (*12*).

To further assess the potential lateral diffusion of transcripts, we investigated the distribution of the expression of 10 different genes with highly enriched expression in the mitral cell layer (MCL),

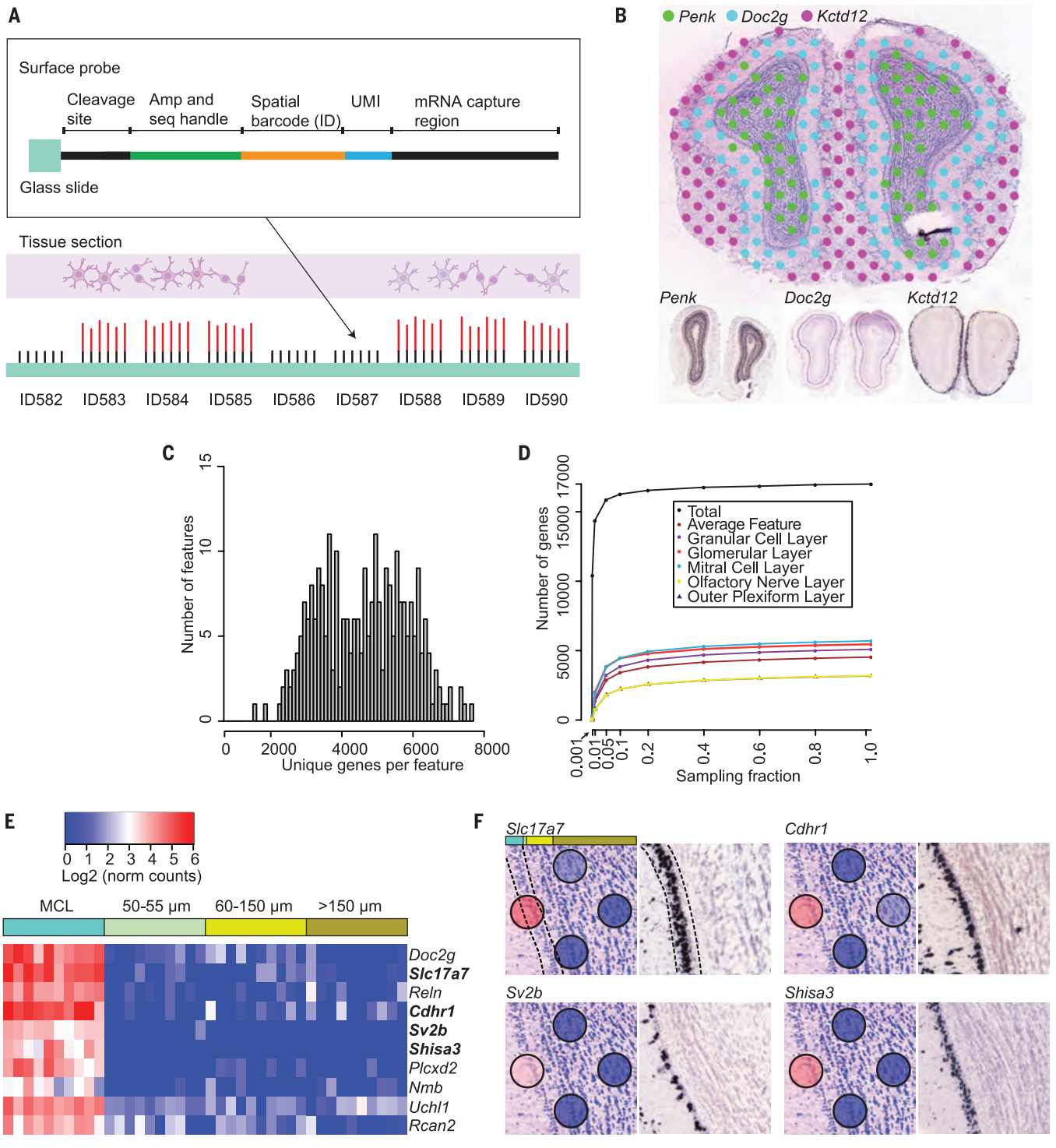


Fig. 2. Spatially resolved gene expression. (**A**) Each array feature contains unique DNA-barcoded probes containing a cleavage site, a T7 amplification and sequencing handle, a spatial barcode, a unique molecular identifier (UMI), and an oligo(dT) VN-capture region, where V is anything but T and where N is any nucleotide. cDNA (red) is generated from captured mRNA by reverse transcription. (**B**) Visualization of the expression of three genes by spatial transcriptomics (top) and in situ hybridization (bottom). *Penk* and *Kctd12* in situ images are from the Allen Institute. Cutoff normalized counts, *Penk*, 8; *Doc2g*, 13; and *Kctd12*, 19. (**C**) Distribution of unique genes per feature under the tissue. (**D**) Number of genes detected for different layers and entire tissue over sequencing depth. (**E**) Lateral diffusion of transcripts from genes enriched in MCL. The genes are expressed in MCL features but are not separable from the background in features adjacent to the MCL. (**F**) Spatial expression and in situ hybridization of four genes in (E). The leftmost feature overlaps the MCL, and the three rightmost features are situated in the GCL. The colored bar depicts the distances from feature center in (E).

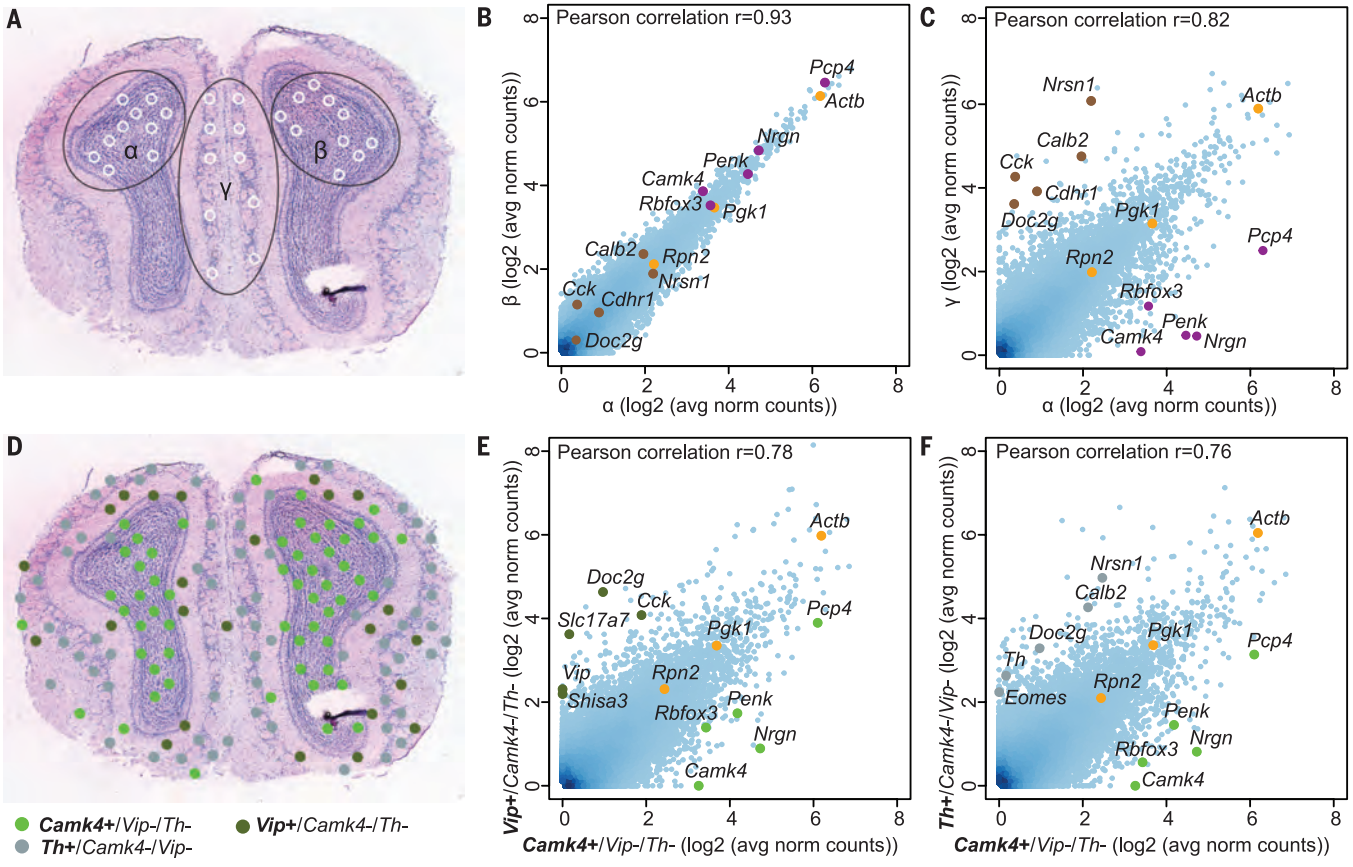


Fig. 3. Visualization and bioinformatics analyses of tissue domains defined by morphology or gene expression profile. (**A**) Ten selected features in areas α (GCL), β (GCL), or γ (GL) are indicated. (**B**) Scatterplot of gene expression in areas α and β shows similar expression of layer-specific genes. Examples of genes are indicated with purple and brown dots. Housekeeping genes are orange. (**C**) Scatterplot of gene expression in areas α and γ shows a difference in gene expression. Examples from the 170 differentially expressed genes are labeled. (**D**) The spatial expression of three interneuron-marker–gene profiles. Ten features with the different expression profiles were randomly selected for differential expression analysis. (**E**) Comparing the 10 *Camk4*$^+$/*Vip*$^-$/*Th*$^-$ features with the 10 *Vip*$^+$/*Camk4*$^-$/*Th*$^-$ features. Examples, out of the 196 differentially expressed genes, are labeled. (**F**) Comparing the 10 *Camk4*$^+$/*Vip*$^-$/*Th*$^-$ features with the 10 *Th*$^+$/*Camk4*$^-$/*Vip*$^-$ features. Examples from the 328 differentially expressed genes are labeled.

and we asked whether they could be detected in the adjacent granular cell layer (GCL). All these genes were confirmed to be highly expressed in the MCL by spatial transcriptomics, but they were undetectable or detected at very low levels within the GCL, even with the border of the feature 0 to 5 μm and the center of the feature 50 to 55 μm from the MCL (Fig. 2, E and F, and fig. S7A). Furthermore, we compared the distribution of transcripts between areas obtained with laser capture microdissection (*6*) where there is no diffusion of transcripts and with spatial transcriptomics features, and we did not find evidence for a difference between these methods in terms of mRNA diffusion (fig. S7, B and C).

A common goal of gene expression analysis of tissues is to define the transcriptome of specific areas. Analysis between homologous regions revealed very similar expression profiles (Fig. 3, A and B, and fig. S8), with no differentially expressed genes. In contrast, comparison of different domains revealed different gene expression profiles (Fig. 3, A and C, and fig. S8). This included genes with previously known restricted expression, such as *Doc2g* in the glomerular layer (GL) and *Penk* in the GCL (*13*), as well as novel layer-specific gene expression profiles (Fig. 3C).

It is valuable to explore the gene expression pattern of populations of cells or tissue domains that can be defined by a combination of markers. Spatial transcriptomics offers an alternative approach that circumvents multiplex labeling and cell isolation. Any combination of presence or absence of expression for a set of genes can be used to define a marker profile of interest for further analysis. Features were selected on the basis of the presence and/or absence of the three interneuron-marker genes *Camk4*, *Th*, and *Vip*. The distribution of features, where one of the genes is expressed alone, is shown in Fig. 3D. Comparing gene expression revealed specific transcriptomes defined by these interneuron-marker profiles (Fig. 3, E and F, and fig. S8).

To further explore gene expression profiles in spatially defined domains within the olfactory bulb, we used principal component analysis (fig. S9) or the t-distributed stochastic neighbor embedding (t-SNE) (*14*, *15*) machine-learning algorithm for dimensionality reduction, followed by hierarchical clustering (Fig. 4A). When placing back the clustered features on the tissue images, it was apparent that each cluster of features largely corresponded to well-defined morphological layers (Fig. 4B). The clusters were then compared with each other, which allowed the identification and visualization of cluster-specific marker genes (fig. S10, A and B). This proved to be an efficient, unbiased way to identify genes with expression enriched in the cell layers of interest. Furthermore, we investigated the gene expression pattern in 10 sections from a total of five animals, as well as the feature-to-feature correlation at the same location in two adjacent sections (fig. S10, C to E).

Analysis of the histology and a set of markers are routine in cancer diagnostics, although analysis of the expression of panels of genes has started to enter the clinic. We asked whether adding a spatial dimension to gene expression analysis may add information in cancer diagnostics and applied spatial transcriptomics to breast cancer biopsies. In Fig. 4, C and D (see also fig. S11, A and B), an area with invasive ductal

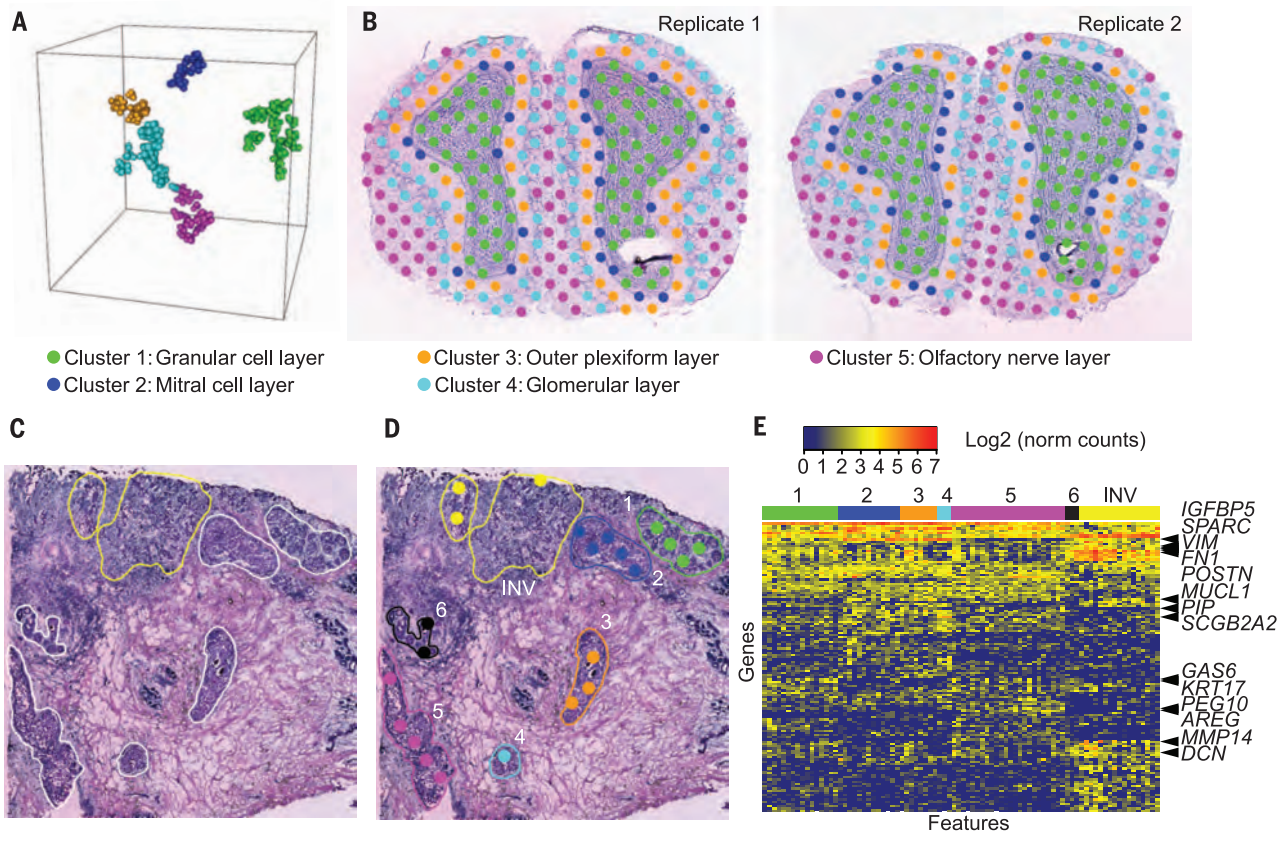


Fig. 4. Comparative analyses of tissue domains. (**A**) t-SNE analysis and hierarchical clustering of 551 features from two replicates creates five distinct clusters. (**B**) The features placed back onto the two tissue images. (**C** and **D**) Histological section of a breast cancer biopsy (C) containing invasive ductal cancer (INV) and six separate areas of ductal cancer in situ (1 to 6), with analyzed spatial transcriptomics features in (D). INV areas without, or with minimal, stromal infiltration were selected. (**E**) Gene expression heat map over the different areas in four adjacent sections (D) and (fig. S11).

cancer, as well as six separate areas of ductal cancer in situ, were identified on the basis of morphological criteria. Spatial transcriptomics analysis of the invasive component revealed high expression of extracellular matrix–associated genes (Fig. 4E). Analysis of the ductal cancer in situ areas revealed a surprisingly high degree of heterogeneity in gene expression between these regions, probably reflecting different subclones, with varying expression of several genes implicated in cancer progression (Fig. 4E and fig. S11C). For example, expression of *KRT17* and *GAS6*, implicated in epithelial-to-mesenchymal transition (*16*, *17*), was high only in areas 1 and 5 (Fig. 4, C to E, and fig S11). Thus, spatial transcriptomics revealed unexpected heterogeneity within a biopsy, which would not be possible to detect with regular transcriptome analysis and which may give more detailed prognostic information.

Spatial transcriptomics calls for only a few extra steps compared with RNA-seq analysis of homogenized tissue, with the benefit of providing spatial information enabling additional levels of analysis. In contrast to standard methods, different domains of the tissue are processed in the same reaction in spatial transcriptomics, which removes technical variation between samples. A unique feature of spatial transcriptomics is that any gene expression profile can be selected to specify a molecularly defined domain for further analysis. Finally, in contrast to when different regions of a tissue are dissected for analysis, the information for the whole section is maintained; hence, the analysis is not limited to the initially selected regions. An individual spatial transcriptomics experiment thus serves as a permanent resource to investigate gene expression patterns for future research questions.

REFERENCES AND NOTES

1. Z. Wang, M. Gerstein, M. Snyder, *Nat. Rev. Genet.* **10**, 57–63 (2009).
2. N. Crosetto, M. Bienko, A. van Oudenaarden, *Nat. Rev. Genet.* **16**, 57–66 (2015).
3. R. Satija, J. A. Farrell, D. Gennert, A. F. Schier, A. Regev, *Nat. Biotechnol.* **33**, 495–502 (2015).
4. P. A. Combs, M. B. Eisen, *PLOS ONE* **8**, e71820 (2013).
5. K. Achim *et al.*, *Nat. Biotechnol.* **33**, 503–509 (2015).
6. Materials and methods are available as supplementary materials on *Science* Online.
7. T. Hashimshony, F. Wagner, N. Sher, I. Yanai, *Cell Reports* **2**, 666–673 (2012).
8. R. N. Van Gelder *et al.*, *Proc. Natl. Acad. Sci. U.S.A.* **87**, 1663–1667 (1990).
9. R. Vassar *et al.*, *Cell* **79**, 981–991 (1994).
10. K. D. Pruitt *et al.*, *Nucleic Acids Res.* **42** (D1), D756–D763 (2014).
11. S. Zechel, P. Zajac, P. Lönnerberg, C. F. Ibáñez, S. Linnarsson, *Genome Biol.* **15**, 486 (2014).
12. D. Grün, A. van Oudenaarden, *Cell* **163**, 799–810 (2015).
13. E. S. Lein *et al.*, *Nature* **445**, 168–176 (2007).
14. A. Mahfouz *et al.*, *Methods* **73**, 79–89 (2015).
15. L. J. P. van der Maaten, G. E. Hinton, *J. Mach. Learn. Res.* **9**, 2579–2605 (2008).
16. M. Kittaneh, A. J. Montero, S. Glück, *Biomarkers Cancer* **5**, 61–70 (2013).
17. C. Gjerdrum *et al.*, *Proc. Natl. Acad. Sci. U.S.A.* **107**, 1124–1129 (2010).

ACKNOWLEDGMENTS

We thank K. Meletis and M. Nilsson for discussions. This study was supported by Knut och Alice Wallenberg Foundation, the Swedish Foundation for Strategic Research, the Swedish Research Council, the Swedish Cancer Society, the Karolinska Institute, Tobias Stiftelsen, Torsten Söderbergs Stiftelse, Ragnar Söderbergs Stiftelse, StratRegen, Åke Wiberg Foundation, and the Jeansson Foundations. P.L.S. was supported by a postdoctoral fellowship from the Swedish Research Council. We thank the Swedish National Genomics Infrastructure hosted at SciLifeLab, as well as the Swedish National Infrastructure for Computing–Uppsala Multidisciplinary Center for Advanced Computational Science and Bioinformatics Long-Term Support for providing sequencing and computational assistance and infrastructure. The sequencing data are deposited at the National Center for Biotechnology Information, NIH, with BioProject ID PRJNA316587. Gene counts and scripts can be downloaded from www.spatialtranscriptomicsresearch.org. P.L.S., F.S., J.L., and J.F. are authors on patents applied for by Spatial Transcriptomics AB covering the technology.

SUPPLEMENTARY MATERIALS

www.sciencemag.org/content/353/6294/78/suppl/DC1
Materials and Methods
Figs. S1 to 11
Tables S1 and S2
References (*18*–*25*)

12 January 2016; accepted 31 May 2016
10.1126/science.aaf2403

www.sciencemag.org/content/353/6294/78/suppl/DC1

Supplementary Materials for

Visualization and analysis of gene expression in tissue sections by spatial transcriptomics

Patrik L. Ståhl, Fredrik Salmén, Sanja Vickovic, Anna Lundmark, José Fernández Navarro, Jens Magnusson, Stefania Giacomello, Michaela Asp, Jakub O. Westholm, Mikael Huss, Annelie Mollbrink, Sten Linnarsson, Simone Codeluppi, Åke Borg, Fredrik Pontén, Paul Igor Costea, Pelin Sahlén, Jan Mulder, Olaf Bergmann, Joakim Lundeberg,* Jonas Frisén

*Corresponding author. Email: joakim.lundeberg@scilifelab.se

Published 1 July 2016, *Science* **353**, 78 (2016)
DOI: 10.1126/science.aaf2403

This PDF file includes

Materials and Methods
Figs. S1 to S11
Tables S1 and S2
References

Supplementary materials

Visualization and analysis of gene expression in tissue sections by spatial transcriptomics

Materials and methods

Outline of the Spatial Transcriptomics workflow

The Spatial Transcriptomics method follows the following workflow: array printing, tissue sectioning, tissue fixation, tissue staining, imaging, pre-permeabilization, permeabilization, cDNA synthesis, tissue removal, probe release, library preparation, sequencing, data processing, data visualization and analysis. When the method refers to separate wells, these wells are created on the glass slide by using a rubber mask (ArrayIT hybridization cassette) to separate the surface into reaction compartments, suitable for the size of the printed arrays, where on-chip reactions can take place. Typically, from tissue types that the protocol has been optimized for, 75% of tissue sections put onto the array will produce high quality data. This is an approximate estimate based on reproducibility between samples of the same type, given the RNA (RIN > 8) and tissue morphology is of good quality. We specify "high quality data" as sample data with an average number of genes per feature above a certain threshold value, as well as correct tissue placement on the spatial array (tissue inside the area, few folded areas and missing pieces etc.). The approximate values differ between different types of samples. For mouse olfactory bulb we require at least 3000 genes per feature at average and at least 90% of the bulb to be intact and

placed within the spatial array. For breast cancer samples we require at least 3000 genes per feature at average in the tumor regions and that all of the tumor regions are placed within the spatial array.

Optimization of the method for a particular tissue requires adjustment of the parameters for permeabilization, usually different times or concentrations (decreased with smaller tissues and increased with larger), as well as adjustment of the section thickness.

Generation of surfaces with poly-T reverse transcription primers

To investigate the feasibility of generating cDNA from mRNA in tissue sections with maintained spatial resolution we immobilized poly-20TVN capture oligonucleotides (IDT) on the surface of Codelink Activated microscope glass slides (#DN01-0025, Surmodics), according to the manufacturer's instructions (Surmodics). The oligonucleotide immobilized on the surface was:

Surface reverse transcription oligonucleotide:

[AmC6]UUUUUGACTCGTAATACGACTCACTATAGGGACACGACGCTCTTCCGATCTN NNNNNNNTTTTTTTTTTTTTTTTTTTVN

Generation of spatially barcoded arrays for Spatial Transcriptomics

For comparing the efficiency of cDNA generation on an array with cDNA generation in solution, and for generation of Spatial Transcriptomics data, we arrayed 1007 capture oligonucleotides with 18-mer unique barcodes, a 9-mer semi-randomized UMI and a poly-20TVN capture region (IDT) onto the surface of Codelink Activated Slides according to the manufacturer's (Surmodics) instructions. The oligonucleotides were immobilized in 100µm features with 200µm center-to-

center distance between the spots. According to the slide manufacturer approximately 200 million oligonucleotides were immobilized in each spot. An area in the top left corner of the array was left blank for the purpose of orientation. Six 6200x6600µm arrays were prepared per glass slide. The oligonucleotides immobilized on the spatially barcoded arrays were:

Surface spatially barcoded oligonucleotides:
[AmC6]UUUUUGACTCGTAATACGACTCACTATAGGGACACGACGCTCTTCCGATCT[18MER_SPATIALBARCODE]WSNNWSNNVTTTTTTTTTTTTTTTTTTTVN

Collection and preparation of olfactory bulbs

For spatial transcriptomics analysis, adult C57BL/6 mice (>2 months old) were euthanized and olfactory bulbs were immediately isolated and snap-frozen in Isopentane (#M32631, Sigma-Aldrich). Tissue was embedded in cold OCT (#4532, Sakura) before sectioning. The olfactory bulb was sectioned on a cryostat at a thickness of 10µm. Sections were mounted onto spatially barcoded arrays or to surfaces with poly-T reverse transcription primers with one section per well. For smFISH, sections were mounted on cover glasses and for LCM, sections were mounted onto MMI Tool membrane (MMI AG, Glattburg, Switzerland).
For in situ hybridization, euthanized mice were transcardially perfused with PBS (#SH30378.02, GE Healthcare Life Sciences) followed by 4% formaldehyde (#F1635, Sigma-Aldrich). Brains were post-fixed in 4% formaldehyde over-night. Vibratome-sections (25µm) were cut and mounted on glass slides (#J1800AMNZ, Fisher Scientific).

Collection and preparation of breast cancer biopsy

The biopsy was collected and snap frozen. Tissue was embedded in cold OCT before sectioning. The biopsy was sectioned on a cryostat at a thickness of 16µm. Every forth section was mounted onto spatially barcoded arrays with one section per well.

Staining and imaging

Sections were fixed for 10 minutes in neutral formaldehyde solution, diluted 1:9 from 36.5 - 38.0% stock solution (#F8775, Sigma-Aldrich) in 1xPBS (#09-9400, Medicago). Directly following fixation, the formaldehyde was washed away with 1xPBS followed by addition of Propan-2-ol (#A461-1, Fisher Scientific), sections for smFISH were stored at -80°C until processed. For Spatial Transcriptomics experiments and LCM experiments, sections were stained with Mayer's Hematoxylin (#S3309, Dako) and Bluing buffer (#CS702, Dako) followed by Eosin (#HT110216, Sigma-Aldrich) in Tris-base (0.45M Tris, 0.5M Acetic acid, pH 6.0). Sections were rinsed, and for Spatial Transcriptomics experiments, dried sections were mounted with 85% Glycerol (#104094, Merck Millipore) and covered with a coverslip (#BB024060A1, Menzel-Gläser).

Bright field imaging was carried out using the Metafer Slide Scanning Platform (Metasystems). Raw images were stitched together with the VSlide software (Metasystems). Images were visualized and extracted as .jpeg.

Permeabilization and reverse transcription

For each well, corresponding to each sub-array with a section, 70µl of 1x Exonuclease I Reaction Buffer (#B0293S, NEB) with 0.19µg/µl BSA (#B9000S, NEB) was added and incubated at 37°C

for 30 minutes. Each well was washed with 100µl 0.1x SSC, diluted in deionized water from stock solution (#S6639, Sigma-Aldrich). Next, 70µl of 0.1% pepsin (#P7000-25G, Sigma-Aldrich) dissolved in 0.1M HCl (#318965-1000ML, Sigma-Aldrich) was added to each well and incubated at 37°C for 10 minutes. Each well was washed as previously described and 70µl of reverse transcription mix was added to each well and incubated overnight (ON). For spatially barcoded arrays belonging to samples intended for sequencing, the reverse transcription mix contained 1x First Strand Buffer (#18080-044, Invitrogen), 5mM DTT (#18080-044, Invitrogen), 500µM of each dNTP (#R0192, Fisher Scientific), 0.19µg/µl BSA, 50ng/µl Actinomycin D (#A1410-2MG, Sigma-Aldrich), 1% DMSO (#472301-500ML, Sigma-Aldrich), 20U/µl Superscript III (#18080-04, Invitrogen) and 2U/µl RNaseOUT (#10777-019, Invitrogen). For spatially barcoded arrays and surfaces with poly-T reverse transcription primer intended for generation of fluorescent cDNA footprints, the reverse transcription mix contained the same reagents as above except for 500µM of each dATP/dGTP/dTTP, 12.5µM of dCTP , 25µM of Cyanine 3-dCTP (#NEL576001EA, PerkinElmer). For experiments optimizing the conditions for permeabilization the permeabilization was carried out for 0, 2, 10 and 30 minutes. For experiments optimizing the conditions for cDNA synthesis the cDNA synthesis was carried out for 1 hour, 3 hours, 6 hours and overnight.

To degrade and remove mouse tissue, 70µl Proteinase K (#19131, Qiagen) and PKD Buffer (pH 7.5, according to the manufacturer, #1034963, Qiagen), at a ratio of 1:7, were added to each well and incubated at 56°C for 1 hour. After the incubation, slides washed with 2x SSC with 0.1% SDS at 50°C (#71736-100ML, Sigma-Aldrich) followed by 0.2x SSC and 0.1x SSC at room temperature (RT) and finally spin-dried. For the breast cancer biopsy, the tissue was incubated in

1:100 β-Mercaptoethanol (#444203, CALBIOCHEM) in RLT buffer (#79216, Qiagen) at 56°C for 1 hour before the Proteinase K step.

cDNA library preparation for sequencing

For each well, 70µl of release mix containing 1.1x Second Strand Buffer (#10812-014, Invitrogen), 8.75µM of each dNTP, 0.20µg/µl BSA and 0.1U/µl USER Enzyme (#M5505, NEB) was added and incubated at 37°C for 1-2 hour and 65µl from each well were collected. 5µl of second strand mix containing 2.7x First Strand Buffer, 3.7U/µl DNA polymerase I (#18010-017, Invitrogen) and 0.18U/µl RNaseH (#18021-014, Invitrogen) was added and samples were incubated at 16°C for 2 hours, 5µl T4 DNA polymerase /#M0203S, NEB) was added and samples were incubated at 16°C for another 20 minutes. 25µl of deionized water or 80mM EDTA (#15575-038, Invitrogen) was added and purified using Agencourt RNAClean XP beads (#A63987, Beckman Coulter) according to the manufacturer's protocol eluted into deionized water. 5.6µl of the samples were mixed with 10.4µl In Vitro Transcription mix with a final content of 1x T7 Reaction Buffer (#AM1333, Ambion), 7.5mM of each NTP (#AM1333, Ambion), 1x T7 Enzyme Mix (#AM1333, Ambion) and 1U/µl SUPERaseIN (#AM2694, Ambion). Samples were incubated at 37°C for 14 hours.

The samples were purified using Agencourt RNAClean XP beads according to the manufacturer's protocol and eluted into 10µl deionized water. The amount and average fragment length of amplified RNA (aRNA) was determined by using the RNA 6000 Pico Kit (#5067-1513, Agilent) with a 2100 Bioanalyzer (Agilent) according to the manufacturer's protocol. The remaining sample and 2.5µl Ligation adapter (IDT) was added to a final concentration of 0.71µM. Samples were heated at 70°C for 2 min. then placed on ice before 4.5µl ligation mix was added to a final

content of 1x T4 RNA Ligase Reaction Buffer (#B0216L, NEB), 20U/µl T4 RNA Ligase2, truncated (#M0242L, NEB), 4U/µl RNase Inhibitor, Murine (#M0314L, NEB) and 0.5µM Ligation Adapter. Samples were incubated at 25°C for 1 hour. The samples were purified using Agencourt RNAClean XP beads according to the protocol previously described and mixed with 1µl RT-primer (IDT) to a final concentration of 1.7µM and 1µl dNTPs and a final concentration 0.83mM of each dNTP. Samples were heated at 65°C for 5 min and then placed on ice, 8µl reverse transcription mix was added to a final content of 1x First Strand Buffer, 0.05M DTT, 500µM of each dNTP, 1mM RT-primer, 10U/µl Superscript III and 2U/µl RNaseOUT. Samples were incubated at 50°C for 1 hour before placed on ice and the samples were subsequently purified using Agencourt RNAClean XP beads according to the protocol previously described. A total reaction volume of 10µl containing 1xKAPA HiFi HotStart ReadyMix (#KK2601, KAPA Biosystems), 1x EVA green (#31000, Biotium), 0.5µM PCR InPE1.0 (Eurofins), 0.01µM PCR InPE2.0 (Eurofins), 0.5µM PCR Index (Eurofins) and 2µl purified cDNA were amplified by qPCR with the following protocol: 98°C for 3 minutes, followed by cycling at 98°C for 20 seconds, 60°C for 30 seconds and 72°C for 30 seconds. After determining the amount of cycles needed based on the qPCR, the samples were amplified in a total reaction volume of 25µl. The libraries were purified as described previously (*18*) and samples were eluted in 20µl elution buffer (#19086, Qiagen) and the average fragment length of finished libraries was determined by using the DNA 1000 Kit (#5067-1504, Agilent) with a 2100 Bioanalyzer according to the manufacturer's protocol. The concentration of the finished libraries was determined with Qubit dsDNA HS Assay Kit (#Q32854, Life Technologies) according to the manufacturer's protocol. Finished libraries were diluted to 4nM and sequenced on the Illumina NextSeq platform using paired-end sequencing according to the manufacturer's protocol. Typically, 31 or 51 bases were

sequenced on read one, and 121 or 101 bases were sequenced on read two. The oligonucleotides used during library preparation were:

Ligation adapter:

[rApp]AGATCGGAAGAGCACACGTCTGAACTCCAGTCAC[ddC]

Second reverse transcription primer:

GTGACTGGAGTTCAGACGTGTGCTCTTCCGA

PCR primer InPE1.0:

AATGATACGGCGACCACCGAGATCTACACTCTTTCCCTACACGACGCTCTTCCGATCT

PCR primer InPE2.0:

GTGACTGGAGTTCAGACGTGTGCTCTTCCGATCT

PCR Index primer:

CAAGCAGAAGACGGCATACGAGATXXXXXXGTGACTGGAGTTC

Fluorescent imaging and image alignment

For spatially barcoded arrays belonging to samples intended for sequencing where barcoded cDNA had been released, 70µl of hybridization mix containing 0.96x PBS, 0.2µM Cy3_anti_A_probe (Eurofins) and 0.2µM Cy3_anti_Frame_probe (Eurofins) was added and incubated at RT for 10 minutes. Each well was washed with 100µl 0.1x SSC, then 2x SSC with 0.1% SDS at 50°C for 10 minutes, 0.2x SSC at RT for 1 minute, 0.1x SSC at RT for 1 minute and finally spin-dried. Both spatially barcoded arrays belonging to samples intended for sequencing, and spatially barcoded arrays and surfaces with poly-T reverse transcription primer intended to

show fluorescent cDNA footprints were mounted with SlowFade Gold Antifade Reagent (#S36963, Invitrogen) and covered with a coverslip.

Fluorescent imaging, stitching and image extraction was carried out on the same system and with the same programs as previously described for bright field images. Bright field images and fluorescent images where manually aligned in Adobe Photoshop CS6 (Adobe), by using tissue structures and features visible in both images. The oligonucleotides used for array hybridization were:

Cy3 anti-A probe:

[Cy3]AGATCGGAAGAGCGTCGTGT

Cy3 anti-Frame probe:

[Cy3]GGTACAGAAGCGCGATAGCAG

Estimation of diffusion by fluorescent signal

Signal intensities were measured in ImageJ for six individual cells (fig. S1E, F). All intensities were then corrected and presented as above background level and the distances between the H&E- and Cy3-signals at 10% of the maximum Cy3-signal intensity measured. An example of the measured distance observations is given in fig. S1G. The average diffusion distance at 10% Cy3-signal was estimated and shown in fig. S1H.

Extraction and fragmentation of total RNA

Total RNA was extracted from fresh frozen sections of the mouse main olfactory bulb. Tissue was placed in Lysing Matrix D (#116913050, MP Biomedicals) and was lysed by running the tubes in

a FastPrep (MP Biomedicals). RNA was extracted using the RNeasy Plus Mini Kit (#74134, Qiagen) according to the manufacturer's protocol. Total RNA was fragmented using the NEBNext Magnesium Fragmentation Module (#E6150S, NEB) for 2.5-3 minutes to an average length of 200-300nts according to the manufacturer's protocol. Fragmented RNA was purified with RNeasy MiniElute Cleanup Kit (#74204, Qiagen) according to the fragmentation protocol. The average fragment length of fragmented RNA and RIN values of extracted RNA was determined by using the RNA 6000 Pico Kit with a 2100 Bioanalyzer according to the manufacturer's protocol. The concentration of the finished libraries was determined with Qubit RNA HS Assay Kit (#Q32852, Life technologies) or Qubit RNA BR Assay Kit (#Q10210, Life technologies) according to the manufacturer's protocol.

Total RNA experiment using spatially barcoded arrays

Total RNA experiments were carried out in the same way as for experiments using tissue sections on spatially barcoded arrays intended for sequencing with three exceptions; no tissue was mounted onto the array, the glycerol mounting step and bright field imaging step were skipped, and 300ng of fragmented total RNA from mouse olfactory bulb was added to each well in the reverse transcription step.

In solution cDNA library preparation

Samples with a total volume of 12µl and a concentration of 1.67mM ST-probe mix (equal mix of six unique barcoded probes), 0.83mM of each dNTPs and 140ng fragmented total RNA from mouse main olfactory bulb were prepared. Samples were heated at 65°C for 5 min. After the heating step, samples were placed on ice before 8µl reverse transcription mix was added to a final

content of 1x First Strand Buffer, 0.05M DTT, 500µM of each dNTP, 1mM ST-probe mix, 10U/µl Superscript II (#18064-014, Invitrogen) 2U/µl RNaseOUT and 1mM TS-probe (Exiqon). Samples were incubated at 42°C for 1 hour followed by 70°C for 15 minutes. Libraries were finished and sequenced in the same way as described after the reverse transcription step under "cDNA library preparation for sequencing". The oligonucleotides used during in solution cDNA library preparation were:

In solution reverse transcription primers:

[AmC6]UUUUUGACTCGTAATACGACTCACTATAGGGACACGACGCTCTTCCGATCT[18MER_SPATIALBARCODE]WSNNWSNNVTTTTTTTTTTTTTTTTTTTTVN

Template switching probe (TS-probe):

AGACGTGTGCTCTTCCGATCTNNNNNNNNATrGrG+G (+=LNA, r=ribo-base)

ISH in tissue sections

ISH was performed as described previously (*19*). Labeled probes were produced with DIG RNA labeling kit (#1175025, Roche). DNA template sequences were amplified from mouse olfactory bulb cDNA using PCR primer (IDT) sequences obtained from Allen Brain Atlas, conjugated to the T3 promoter sequence. The oligonucleotides used for *Rbfox3* template amplification were:

Rbfox3 forward primer:

CCAGCTGAATATGCCCCACC

Rbfox3 reverse primer (including T3 promoter):

ATTAACCCTCACTAAAGGGAGGCCGATGGTGTGATGGTAA.

Single molecule fluorescent in situ hybridization

The sections were permeabilized with methanol and incubated for 10 minutes at 70°C in Tris-EDTA (pH 8.0.) Slides were washed twice with 2xSSC and the incubated in hybridization buffer (*20*) containing 250nM fluorescent label probes (LGC Biosearch Technologies) for 4 hours at 38.5°C. Slides were washed four times in 2xSSC, 20% formamide and counterstained with Hoechst. The staining step was followed by a wash in 2xSSC and finally the slides were mounted with Prolong Gold mounting medium (#P36930, ThermoFisher Scientific). Image stacks (0.3µm distance) were acquired using a Nikon Ti-E with motorized stage (Nikon).

The images were analyzed using python with the numpy, scipy.ndimage and scikit-image libraries. Briefly, after background removal using a large kernel gaussian filter, a Laplacian-of-Gaussian was used to enhance the RNA dots. Background objects, significantly larger than the smFISH dots, were removed after image thresholding. The remaining RNA dots were counted in round areas with a diameter of approximately 100µm in GCL, MCL, OPL and GL (3-6 areas per region). The images were stitched, aligned and pseudocolored in Fiji. The count data was compared to Spatial Transcriptomics data in the same regions with the exception that all possibly spots, overlapping only one region in the section, were used.

Laser capture microdissection

Laser capture microdissection was performed with the Olympus IX81 system (Olympus) and utilizing the mmi Cell Tools (MMI). The microdissected pieces were captured onto 0.2 ml white isolation caps for subsequent cDNA synthesis and library preparation. Round areas with a diameter slightly above 100µm were cut from MCL and GCL. This size was chosen in order to mimic the feature size on Spatial Transcriptomics arrays. After capture, 100ul Lysis buffer from

the RNAqueous-Micro Total kit (#AM1931, Ambion) was added to the tubes followed by an incubation for 30 min at 42 °C. The samples were frozen down at -80 °C until further processing. RNA was extracted using kit according to the manufacturer´s protocol. After extraction, the volume was brought down to 2ul using a Speedvac. To each sample, an unique ST-probe (0.1 pmol) was added as well as DTT, 1uM dNTP mix, SuperScript III and RNaseOUT to a final concentration as stated in the standard protocol. Also actinomycin D (dissolved in 10% v/v DMSO) was added, to the same concentration as previously described, and samples were resuspended in 1x First Strand Buffer to a total volume of 10ul. The reverse transcription was performed at 42°C for 60 min followed by a heat inactivation step at 70 °C for 15 minutes. A total RNA experiment on a spatial array was carried out as previously described but with 500ng of fragmented total RNA (per well) from MCF-7 cells. During the release step, the LCM cDNA was spiked in, with a maximum of three samples per well. Libraries for sequencing were carried out as previously described. The oligonucleotides used for LCM cDNA library preparation were:

LCM reverse transcription primers:

[AmC6]UUUUUGACTCGTAATACGACTCACTATAGGGACACGACGCTCTTCCGATCT[18MER_SPATIALBARCODE]WSNNWSNNVTTTTTTTTTTTTTTTTTTTTVN

Sequence alignment and generation of gene expression database

In each pair of reads, the first read contained the spatial barcode and the UMI but no gene information. Read two contained the gene information and was first processed using BWA based quality trimming. In addition, stretches of homopolymers exceeding 15 bases were removed together with the sequence following the homopolymer, and all reads shorter than 28 bases were

discarded. Remaining reads were aligned against the mouse genome (GRCm38) for olfactory bulb samples, and against the human genome (GRCh38) for breast cancer samples, using Bowtie2 (*21*) v2.2.3 with default settings. The number of reads aligning to each gene were counted with htseq-count (*22*) v0.6.1, using RefSeq gene annotations restricted to validated protein coding and non-coding transcripts (transcript_ids starting with "NM_" or "NR_") for olfactory bulb samples, and using ensembl gene annotations for breast cancer samples. Mitochondrial genes, ribosomal sequences and the long-non-coding transcript "Malat1" were removed from the analysis due to high abundance and internal priming. Whenever read two in a read pair was aligned to a gene, the spatial barcode from the corresponding read one was assigned to a barcode in the reference file as described previously (*23*) ("de-multiplexing"). To remove reads that were duplicated during the amplification protocol, a cluster algorithm that sorts the UMIs and iterates over them to create clusters based on minimum hamming distance was used. Finally all information was written to a file to generate a database containing combined gene expression and spatial information.

Comparing libraries and features

The total expression for each gene in a dataset was calculated by adding the reads from each barcode together. Data from the replicates and the library made in solution was normalized using the median ratio normalization method implemented in DESeq2 (*24*), followed by adding a pseudocount of 1 before the data was log2-transformed. For each pair-wise comparison, the Pearson correlation was calculated using all genes expressed in any of the two datasets.

To compare the number of genes at different read depths in each of three samples (ST, total RNA in solution and total RNA on surface), FASTQ files were down-sampled.

Read coverage over an average "meta-gene" was calculated using the script *geneBody_coverage2.py* from the RSeQC suite (*25*).

To display the number of unique genes and transcripts per feature and the coefficient of variation versus the mean expression, 273 features that were covered by at least 50% tissue were selected. All transcripts expressed were used and, except for the amplification duplicate removal (UMI-filtering), no normalization was carried out. To calculate the number of genes and unique reads per feature in selected morphological regions, a subset of features only covered by one region was selected. A total of 37 features from olfactory nerve layer, 41 from glomerular layer, 37 from outer plexiform layer, 13 from mitral cell layer and 60 from granular cell layer were chosen for this purpose. Subsampling was performed as described above.

Spatial gene expression analysis and visualization

The position of features containing genes of interest was plotted in R using the files containing the spatial gene expression information. Only features with more than 1000 genes were used. Samples were normalized as previously described. To display the enriched spatial expression patterns for selected genes, individual cutoffs were applied based on the total expression of the selected gene in the dataset.

To visualize low horizontal diffusion, ten features from MCL and 30 features from GCL at different distance from MCL were selected. Since only ten features could be found at the closest distance, center of feature at 50-55μm from MCL, this number was also chosen for the other areas. From Allen Brain Atlas, ten genes with a specific expression in MCL, OPL and GL but not in GCL were chosen. Data was normalized as previously described. The expression for each feature at the different distances were visualized as a heat map and directly visualized on top of the tissue.

Also, the sum of unique transcripts for all ten genes was also added together to calculate a value in average per feature for each region. The same procedure was repeated for the LCM samples; however, only five samples from each region were obtained.

Differential expression analysis

For analysis of differential expression between selections based on morphology, ten features from each of three regions were selected. Only features with more than 1000 genes were used and data was normalized as previously described. Features in regions α and β were located in the granular cell layer, with one region from each hemisphere. Features in region γ were located in the glomerular layer in both hemispheres. Pair-wise comparisons were carried either by taking the mean expression of each gene over all ten features or by comparing single features directly. Differential expression analysis was carried out using DESeq2. Only genes with a log2-fold change > 1 and an adjusted p-value of < 0.05 were considered to be differentially expressed. For each selection, examples of overexpressed genes were marked in the scatterplot together with three housekeeping genes (*Rpn2, Pgk1* and *Actb*).

For analysis of differential expression between gene-based selections, data was normalized as previously described. Features were selected based on the presence and absence of three interneuron marker genes, *Camk4*, *Vip* and *Th*. A gene was considered present if the expression was 1 or more normalized counts in a feature and absent if the expression was below 1. To ensure that selections with similar sequencing depth were compared, ten random features from each set were selected. Pair-wise comparison and differential expression analysis were carried out as previously described. The three house keeping genes together with examples of overexpressed genes were marked in the scatterplot.

Dimensionality reduction and hierarchical clustering

All features from both replicates covered by at least 50% tissue and expressing 1000 genes were chosen for t-SNE, making up 551 features. All genes present in at least one feature, making up a total of 17,201 genes, were used. Data was normalized as previously described. The Rtsne R package was used to perform dimensionality reduction of the expression data. The separated features were plotted in three dimensions and each feature was assigned to a cluster based on Euclidean distance (ward.D2). To determine the optimal number of clusters, the DIndex method from the NbClust R package was used. Each cluster was assigned a color and the features were plotted in the tissue showing the cluster color. To find cluster-specific marker genes, DESeq2 were used, and each cluster was compared to the rest of the features. Genes with a log2-fold change > 2 and an adjusted p-value < 0.05 were collected in a heat map, making up 532 genes. Examples of these genes were plotted in the tissue with the gene expression values colored from dark blue (low) to yellow (medium) to red (high).

Principal component analysis was carried out on features that contained at least 1000 genes and that only overlapped one morphological region. Thus, 186 out of the 273 features located under the tissue were selected, with 37 from olfactory nerve layer, 41 from glomerular layer, 37 from outer plexiform layer, 13 from mitral cell layer and 58 from granular cell layer. Data was normalized as previously described. Principal component analysis (PCA) was carried out using the prcomp() function in R by using all genes present in at least one feature, making up a total of 16,155 genes. To show some examples of genes that contribute most to the separation, the loadings of example genes were plotted over the PCA plots.

Correlation between individual features in adjacent sections

Replicate 10 and 11 were chosen due to the fact that they were adjacent to each other and that it was possible to find features with the approximate same location. The data was normalized as previously described and Pearson correlations were calculated using all genes present in at least one of the two features that were compared.

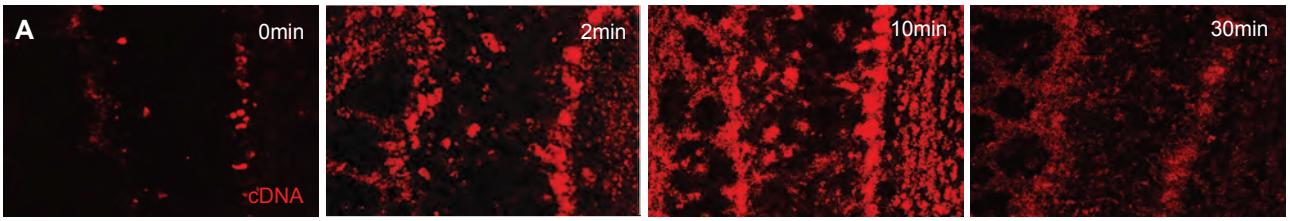
Analysis of breast cancer biopsy

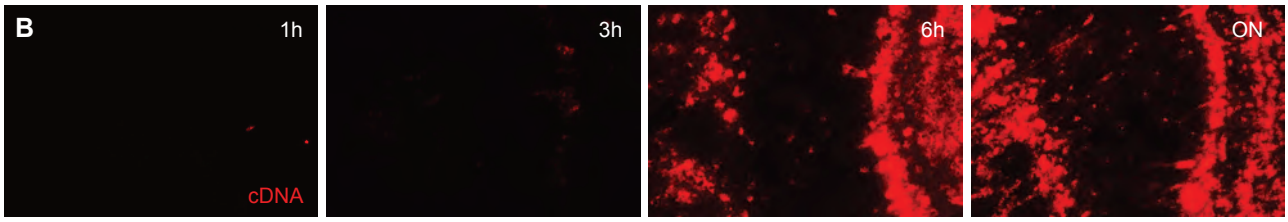
Areas with invasive ductal cancer, as well as areas of ductal cancer in situ were marked by a pathologist. For analysis of differential expression, features from each of the seven regions were selected (in all four tissue sections, Fig. 4C, D, fig. S11A, B). Only features with more than 1000 genes with none or minimal infiltration of stromal cells were used and data was normalized as previously described. Differential expression analysis was carried out using DESeq2. Only genes with a log2-fold change > 2 and an adjusted p-value of < 0.05 (between two regions) were visualized and examples of relevant genes were marked in the heatmaps (Fig. 4E, fig. S11C).

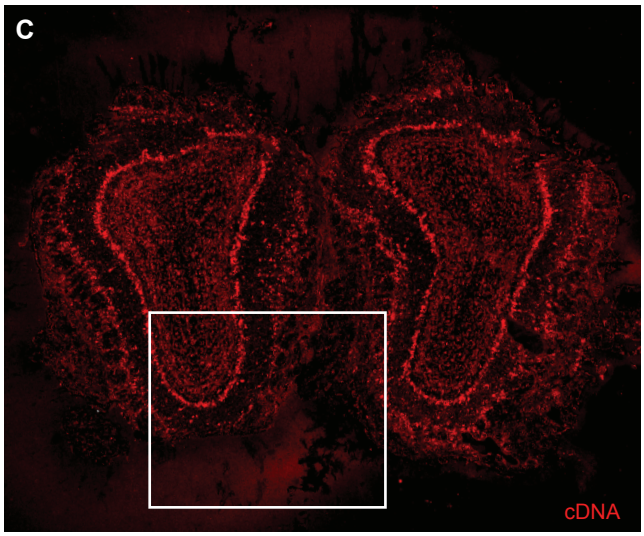
Comparison of Spatial Transcriptomics data and ISH data

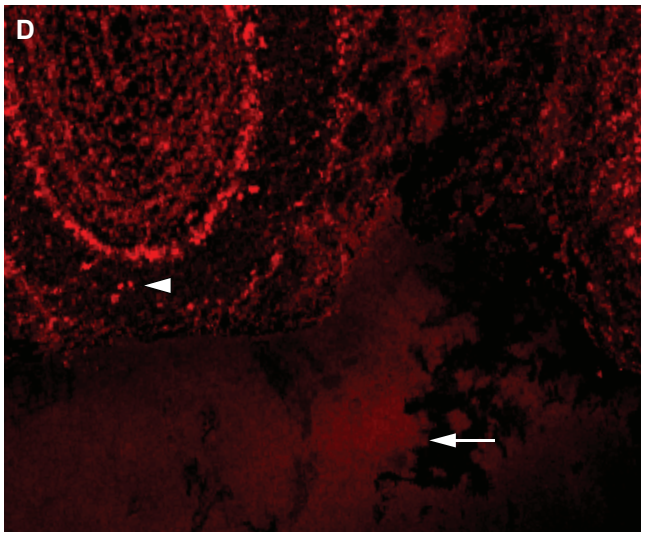
Allen Brain Atlas ISH gene expression data for sagittal sections were downloaded through the API using a modified version of the example script provided at http://api.brain-map.org/examples/doc/structures/download_data.py.html. To compare the number of genes that could be detected with Spatial Transcriptomics versus Allen Brain Atlas, genes with expression energy of at least 1 (default) in Allen Brain Atlas, and 10 unique transcripts (slightly above one detected transcript per million mapped) from Spatial Transcriptomics RNA-seq data were used. Genes that were only detected with one of the methods, as well as the genes that could be detected

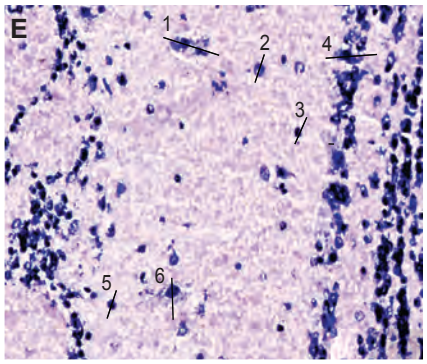
with both methods are presented as a Venn diagram. The expression and number of genes that are specifically detected with only one of the method are showed in scatterplots. The biological functions of the 1070 ABA-specific genes were determined by using Panther and DAVID.

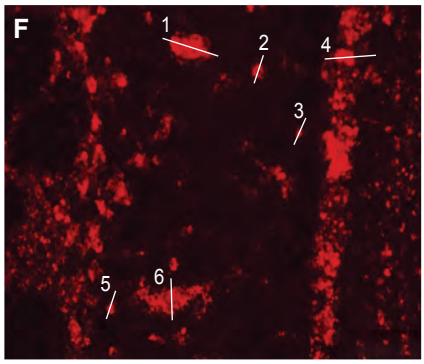

A
0min
2min
10min
30min
cDNA

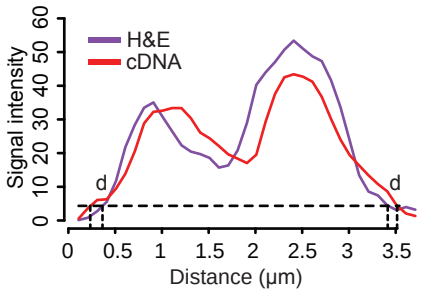

B
1h
3h
6h
ON
cDNA


C
cDNA


D


E
1
2
3
4
5
6


F
1
2
3
4
5
6


G
H&E
cDNA
Signal intensity
0 10 20 30 40 50 60
d
d
0 0.5 1 1.5 2 2.5 3 3.5
Distance (μm)

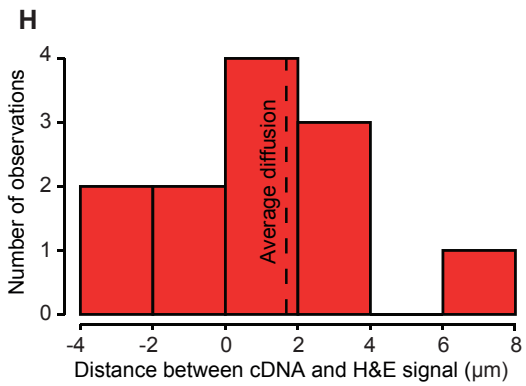

H
Number of observations
0 1 2 3 4
Average diffusion
-4 -2 0 2 4 6 8
Distance between cDNA and H&E signal (μm)

Fig. S1. Spatially localized cDNA synthesis from a tissue section on an oligo(dT)-array

(A) A time series showing the fluorescent cDNA footprint corresponding to varying pepsin permeabilization incubation times. The signal increases from 0 minutes, through 2 minutes to 10 minutes, and has started to blur out at 30 minutes.

(B) A times series showing the fluorescent cDNA footprint corresponding to varying incubation times for cDNA synthesis. The amount of cDNA increases from 1 hour, through 3 hours to 6 hours, and remains at this intensity over night (ON).

(C) Non-specific fluorescent cDNA signal can be observed around the edges of the tissue. This signal can be linked to diffusion of RNA from the edges of the section. In a magnified image it can be observed that this does not affect the spatial restriction of the fluorescent cDNA signal under the tissue.

(D) Magnification of box in **(C)**. Arrowhead indicates cDNA under the tissue with preserved spatial restriction. Arrow indicates cDNA synthesized from RNA diffused from the edges of the tissue.

(E, F) Measuring areas for six cells, marked in H&E- (black lines) and Cy3-channels (white lines) respectively. The measuring areas include both cells and connective tissue in order to quantify the diffusion distance.

(G) As an example, signal intensities for cell 2 in both channels with depicted distance (d) at 10% of Cy3-signal intensity, is shown.

(H) Histogram showing the observed distances, where Cy3-signal can be detected outside the cells.

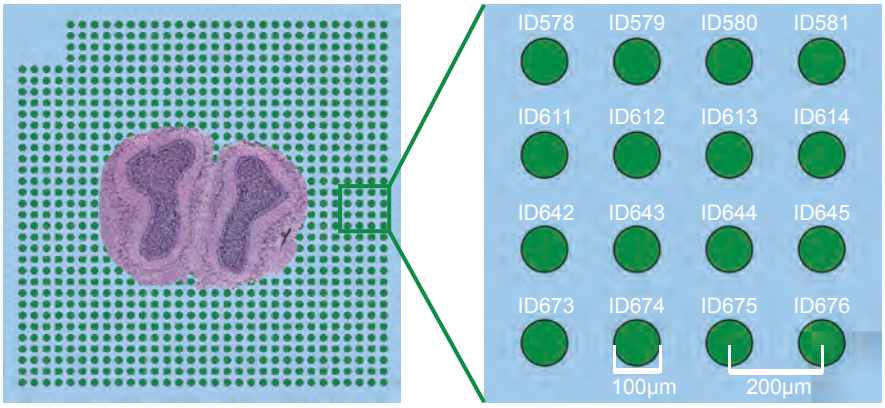


Fig. S2. Spatially barcoded array

Layout of barcoded capture probes on the spatially barcoded array overlaid with a tissue section. The diameter of each spot is 100µm and the spot center to center distance is 200µm.

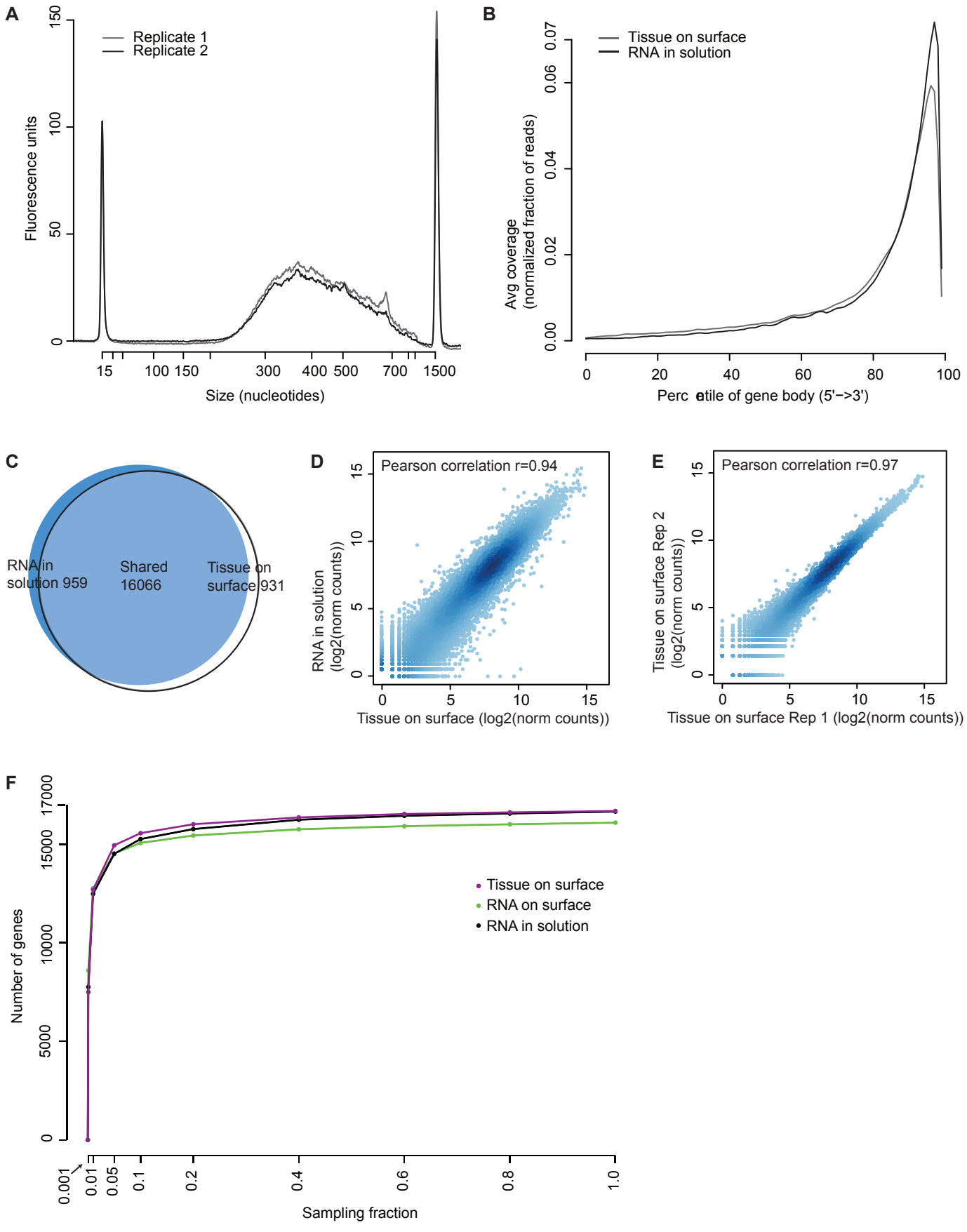

A
Replicate 1
Replicate 2
Fluorescence units
0
50
100
150
15
100 150
300
400 500
700
1500
Size (nucleotides)
B
Tissue on surface
RNA in solution
Avg coverage
(normalized fraction of reads)
0.00
0.02
0.04
0.06
0.07
0
20
40
60
80
100
Perc entile of gene body (5'−>3')
C
RNA in
solution 959
Shared
16066
Tissue on
surface 931
D
Pearson correlation r=0.94
RNA in solution
(log2(norm counts))
0
5
10
15
Tissue on surface (log2(norm counts))
E
Pearson correlation r=0.97
Tissue on surface Rep 2
(log2(norm counts))
Tissue on surface Rep 1 (log2(norm counts))
F
Number of genes
0
5000
10000
15000
17000
Tissue on surface
RNA on surface
RNA in solution
0.001
0.01
0.05
0.1
0.2
0.4
0.6
0.8
1.0
Sampling fraction

Fig. S3. Comparison of cDNA libraries generated in solution or on the surface of a spatially barcoded array

(A) Bioanalyzer DNA 1000 (Agilent) trace, showing average size of libraries generated from cDNA synthesized from tissue on a spatial array.

(B) Read coverage over an average "meta gene" shows a distinct peak at the 3'-end. Read coverage from an RNA in solution library and a tissue on array library are overlaid.

(C) Venn diagram of genes detected in extracted total RNA in solution and a tissue section processed on the surface of an array.

(D) Scatterplot of gene expression for an in-solution and an array sample. The samples show an even representation of highly and lowly expressed genes.

(E) Scatterplot of gene expression between two replicates processed on an array.

(F) Diversity of transcriptome data from extracted total RNA from tissue processed in solution, tissue section processed on spatially barcoded array and extracted total RNA from tissue processed on spatially barcoded array.

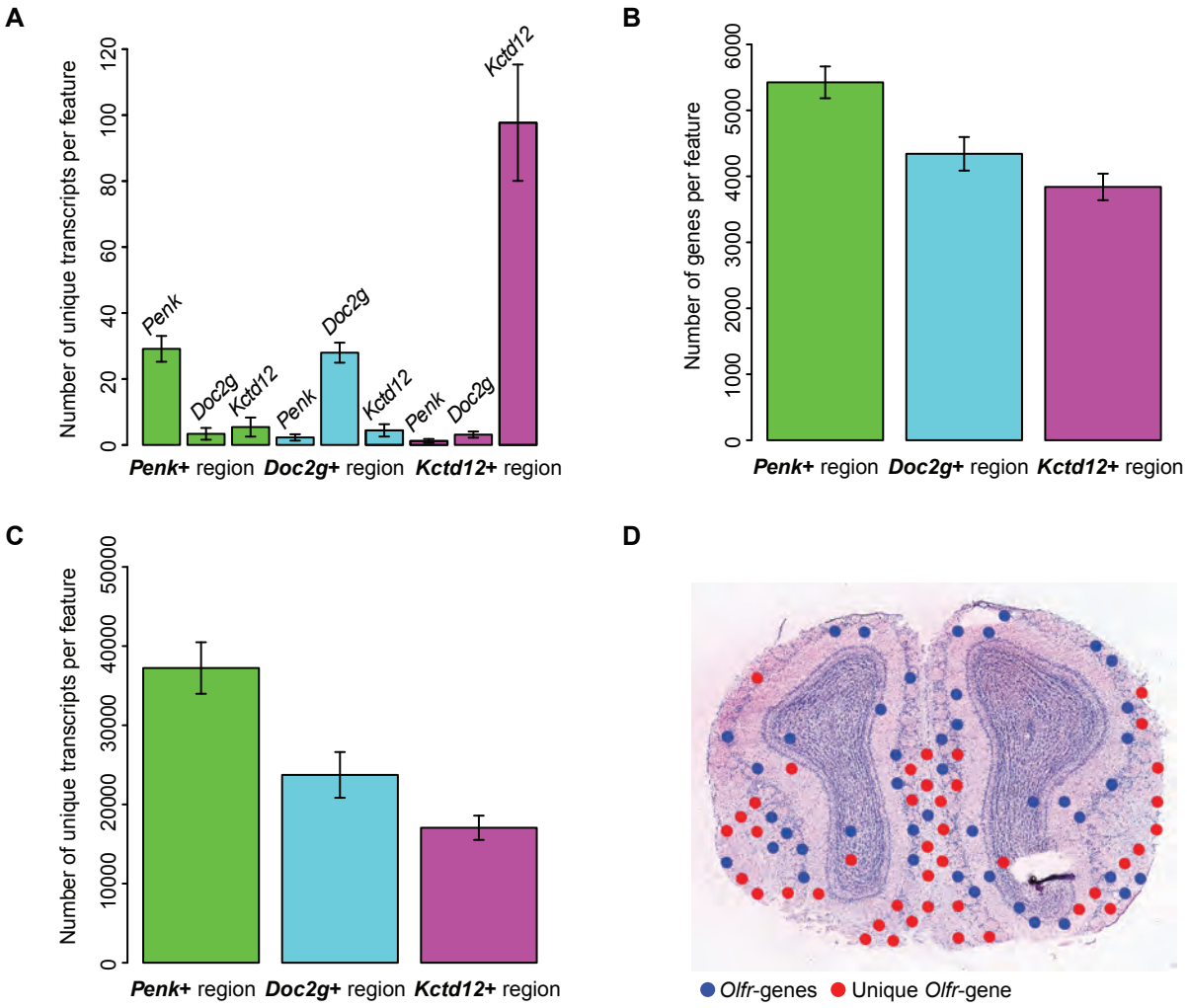


Fig. S4. Expression and distribution of *Penk*, *Doc2g*, *Kctd12* and *Olfr*-genes

(A) Average expression and distribution of *Penk*, *Doc2g* and *Kctd12* in regions that are enriched for the same threee genes as shown in **Fig. 2B**. Error bars represent standard deviation.

(B) Average number of genes in each of the three regions enriched for *Penk, Doc2g* or *Kctd12* as shown in **Fig. 2B**. Error bars represent standard deviation.

(C) Average number of unique transcripts in each of the three regions enriched for *Penk*, *Doc2g* or *Kctd12* as shown in **Fig. 2B**. Error bars represent standard deviation.

(D) Distribution of features with detected lowly expressed olfactory receptor transcripts (*Olfr*). Blue denotes a feature where *Olfr*-genes are detected. Red denotes a feature where a unique *Olfr*-gene to this tissue sample is detected. In total 77 unique *Olfr* transcript types were detected across 57 different features.

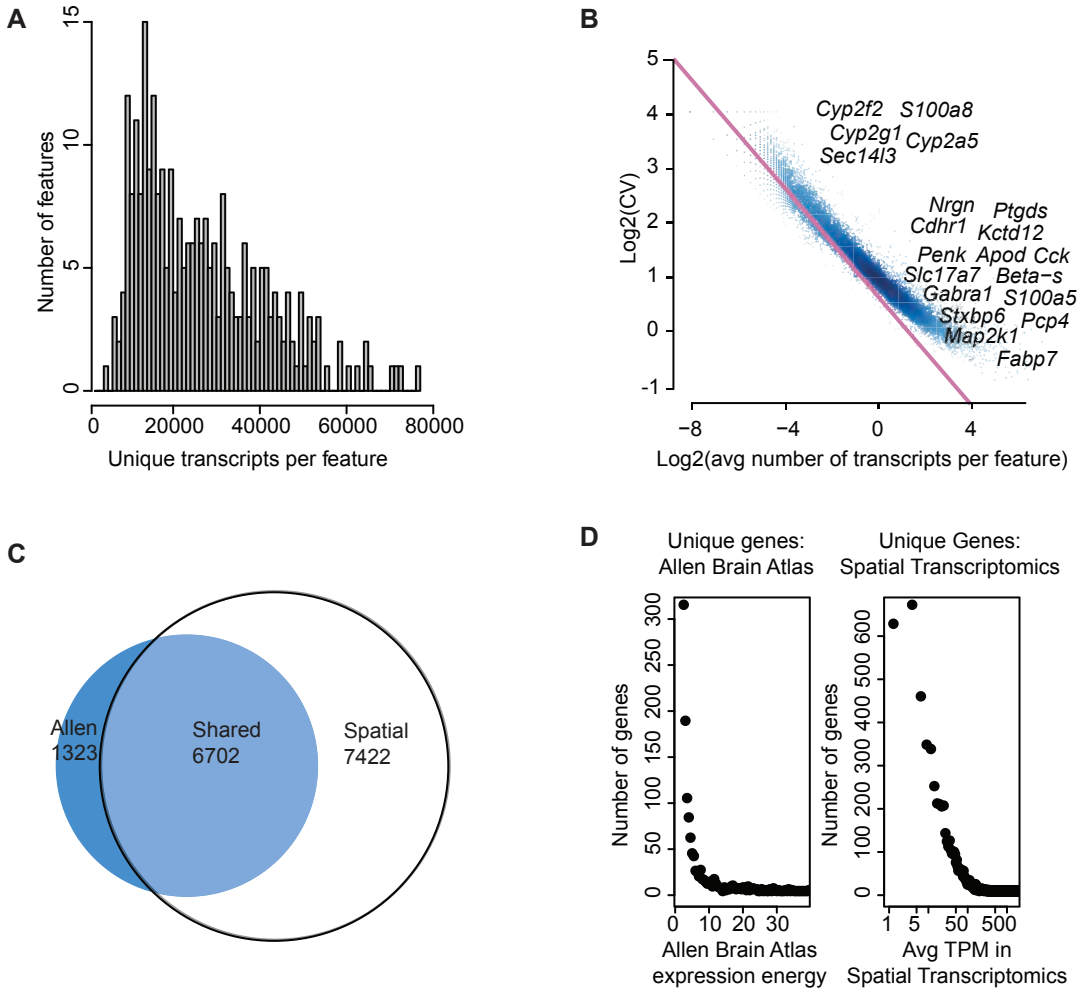


Fig. S5. Capture of gene expression data by Spatial Transcriptomics compared to ISH database

(A) Distribution of unique transcripts captured per feature (UMI-filtered) under the tissue during an experiment on the Spatially barcoded array, in which 273 features were covered by tissue.

(B) CV over average expression per feature for UMI-filtered transcripts. Red line shows theoretical Poisson distribution. Example genes with divergent variation are labeled.

(C) Comparison of genes detected in Allen Brain Atlas (ABA) ISH data and Spatial Transcriptomics RNA-seq data. Using the default expression cutoff (for differential expression analysis) of 1, for the ABA dataset and a cutoff of 10 unique transcripts per gene (corresponding to approximately 1 transcript per million mapped) for Spatial Transcriptomics RNA-seq data, the Spatial Transcriptomics RNA-seq data detects almost twice as many genes.
Of the 1323 genes detected in mouse olfactory bulb in the ABA but not with Spatial Transcriptomics, 253 could not be identified in RefSeq, used for annotation in Spatial Transcriptomics, despite searching for gene aliases via information in the Allen API, or mapping ABA probe sequences (also retrieved from the Allen API) to RefSeq mRNA annotations. Of the remaining 1070 ABA-specific genes that could be identified, 630 had no evidence of expression (no observed reads) in Spatial Transcriptomics, and 440 had expression bellow the defined threshold. In terms of biological function, transcription factor genes (especially homeobox genes) and immune genes were overrepresented in this set of 1070 ABA-specific genes.
(D) Number of genes that are detected with one of the method but not with the other, against the expression values. Most of the genes that are detected using only one of the technologies are weakly detected with the other technology; ~90% of the genes that are not detected with Spatial Transcriptomics have an expression energy below 10 in ABA, while ~85% of the genes not detected in ABA have a mean TPM below the overall mean TPM in Spatial Transcriptomics.

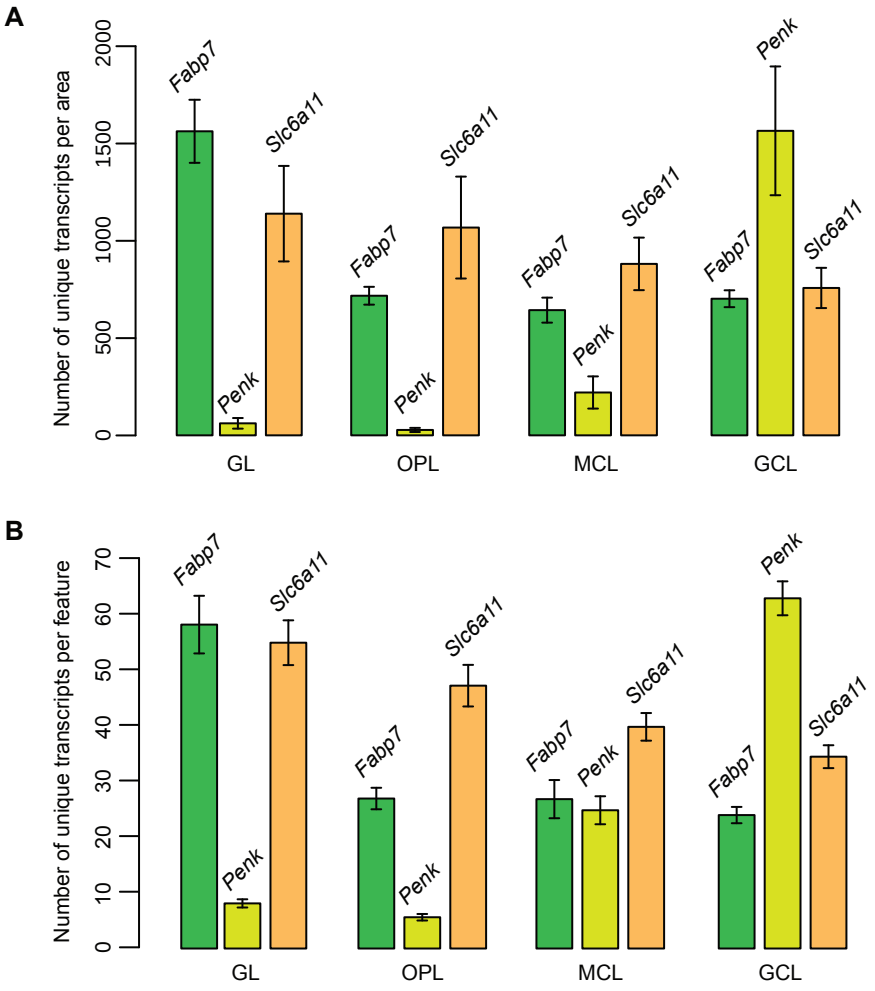


Fig. S6. Count data for smFISH and Spatial Transcriptomics

(A) The average number of unique transcripts, for *Penk*, *Fabp7* and *Slc6a11*, detected in GL, OPL, MCL and GCL with smFISH. Error bars represent standard deviation.

(B) The average number of unique transcripts, for *Penk*, *Fabp7* and *Slc6a11*, detected in GL, OPL, MCL and GCL with Spatial Transcriptomics. The expression patterns show similarity to smFISH **(A)** with a sensitivity of 6.9±1.5%. Error bars represent standard deviation.

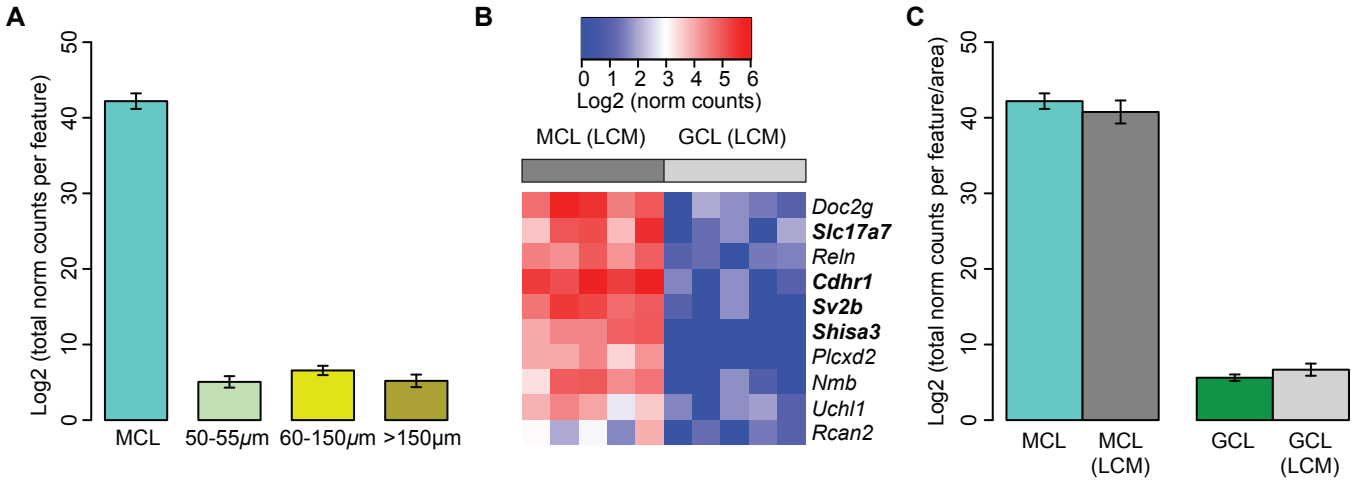


Fig. S7. Expression and distribution of layer-specific marker-genes

(A) The average sum of unique transcripts, for all ten genes (**Fig. 2E**), per feature in MCL and in GCL at various distances from MCL. Data shows very little expression in GCL compared to MCL with no significant difference in expression in relation to distance from MCL. Error bars represent standard deviation.

(B) LCM data was obtained from round areas with a diameter of ~100µm. Heatmap, from these experiments, showing expression of genes enriched in MCL. The genes are highly expressed in MCL, but show non-or low expression in GCL with similar distribution as detected with Spatial Transcriptomics (**Fig. 2E**).

(C) The average sum of unique transcripts, for all ten layer-specific marker-genes, per feature or area in MCL and GCL, detected with Spatial Transcriptomics (**Fig. 2E**) or LCM **(A)**. The expression profiles are very similar using both methods with very few transcripts detected in GCL as compared to MCL. Error bars represent standard deviation.

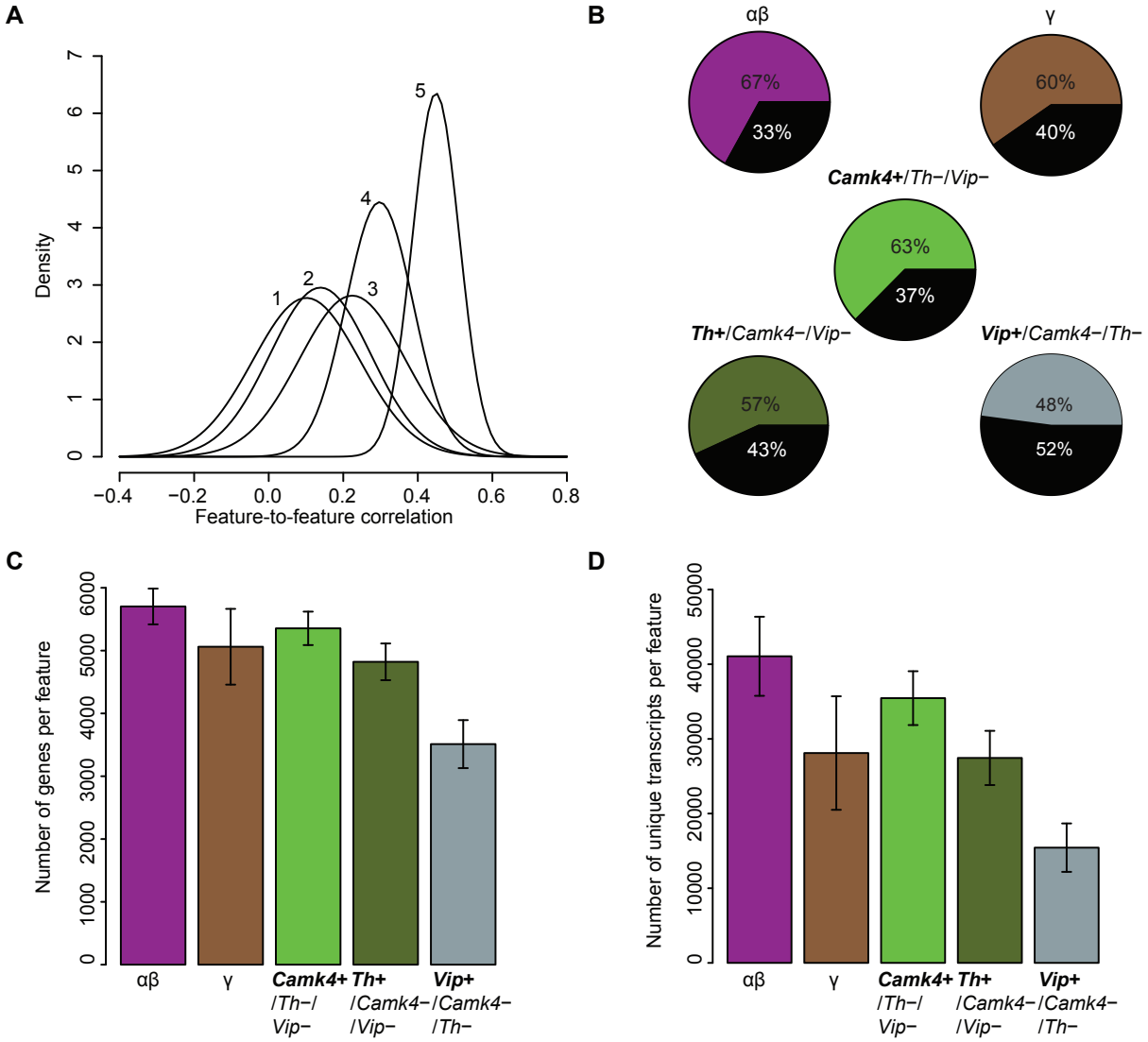


Fig. S8. Feature-to-feature correlation and gene detection for different regions

(A) Normal distribution of Pearson correlations between individual features within the same morphological region or between features within different morphological or marker-based regions. Correlations; 1 (***Vip***+/*Camk4*-/*Th*- to ***Th***+/*Camk4*-/*Vip*-): r=0.10 ± 0.14, 2 (***Camk4***+/*Vip*-/*Th*- to ***Vip***+/*Camk4*-/*Th*-): r=0.14 ± 0.14, 3 (***Camk4***+/*Vip*-/*Th*- to ***Th***+/*Camk4*-/*Vip*-): r=0.22 ± 0.14, 4 (α to ϒ): r=0.30 ± 0.06, 5 (α to β): r=0.45 ± 0.09.

(B) The average percentage (colored parts) of genes detected in both of two individual features from the same morphological or marker-based regions. The black parts show the average percentage of genes that are not detected in both features.

(C) Average number of genes in each of the five regions as shown in **Fig. 3A, D**. Error bars represent standard deviation.

(D) Average number of unique transcripts in each of the five regions as shown in **Fig. 3A, D**. Error bars represent standard deviation.

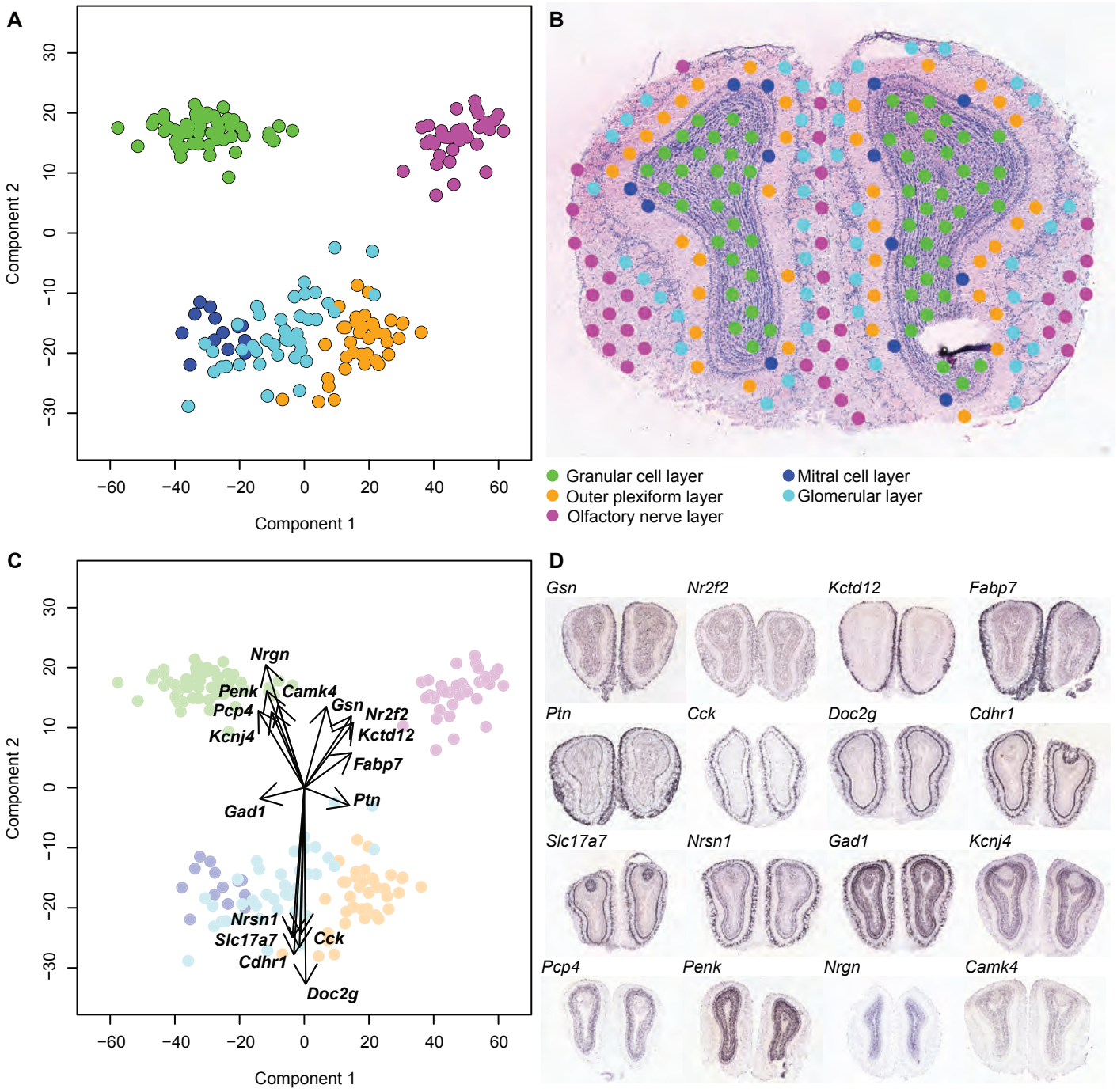


Fig. S9. Principal component analysis of tissue domains

(A) A principal component analysis (PCA) of gene expression profiles from 186 features taken from five regions under the tissue. Each dot is colored accordingly to which region it was selected from.

(B) The position of each feature that was selected for PCA.

(C) PCA bi-plot showing some of the genes (loadings) that contribute the most to the separation.

(D) ISH images of the genes detected as driving the separation in the PCA. ISH images are from the Allen Institute.

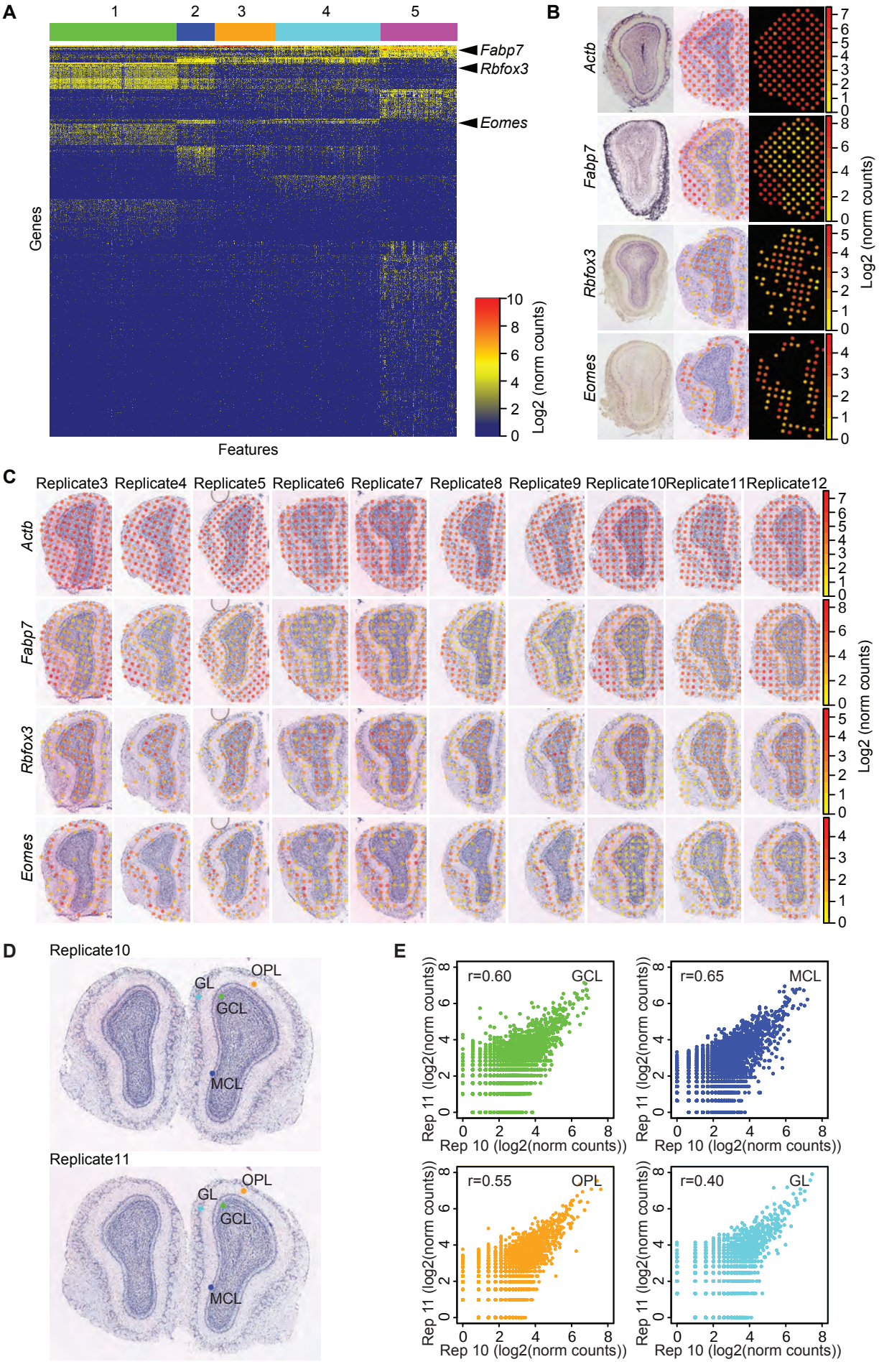

A
1
2
3
4
5
Fabp7
Rbfox3
Eomes
Genes
Features
Log2 (norm counts)
B
Actb
Fabp7
Rbfox3
Eomes
Log2 (norm counts)
C
Replicate3
Replicate4
Replicate5
Replicate6
Replicate7
Replicate8
Replicate9
Replicate10
Replicate11
Replicate12
Actb
Fabp7
Rbfox3
Eomes
Log2 (norm counts)
D
Replicate10
OPL
GL
GCL
MCL
Replicate11
OPL
GL
GCL
MCL
E
r=0.60
GCL
r=0.65
MCL
r=0.55
OPL
r=0.40
GL
Rep 11 (log2(norm counts))
Rep 10 (log2(norm counts))

Fig. S10. Expression patterns of cluster-specific marker-genes

(A) Heatmap showing expression patterns of 532 cluster-specific marker-genes from the tissue sections shown in **Fig 4B**.

(B) Spatially resolved expression profiles of cluster-specific marker-genes, *Fabp7*, *Rbfox3* and *Eomes* identified in **(A)**, as well as house keeper *Actb* (the two right panels) and ISH-images from the Allen Brain Atlas as reference (the left panel). The spatial expression patterns show high similarity between Spatial Transcriptomics and ISH.

(C) Spatially resolved expression profiles in ten tissue sections (replicates) taken from five different animals. The spatial expression patterns show high similarity between replicates.

(D) The position of four selected features, from different morphological regions (GCL, MCL, OPL and GL), in each of two adjacent tissue sections (Replicate 10 and 11) that are located at the approximate same positions in each of the sections.

(E) Scatterplot with Pearson correlations between features shown in **(D)**. The correlations range from 0.40-0.65 between individual features located at the approximate same positions in each of the two adjacent sections.

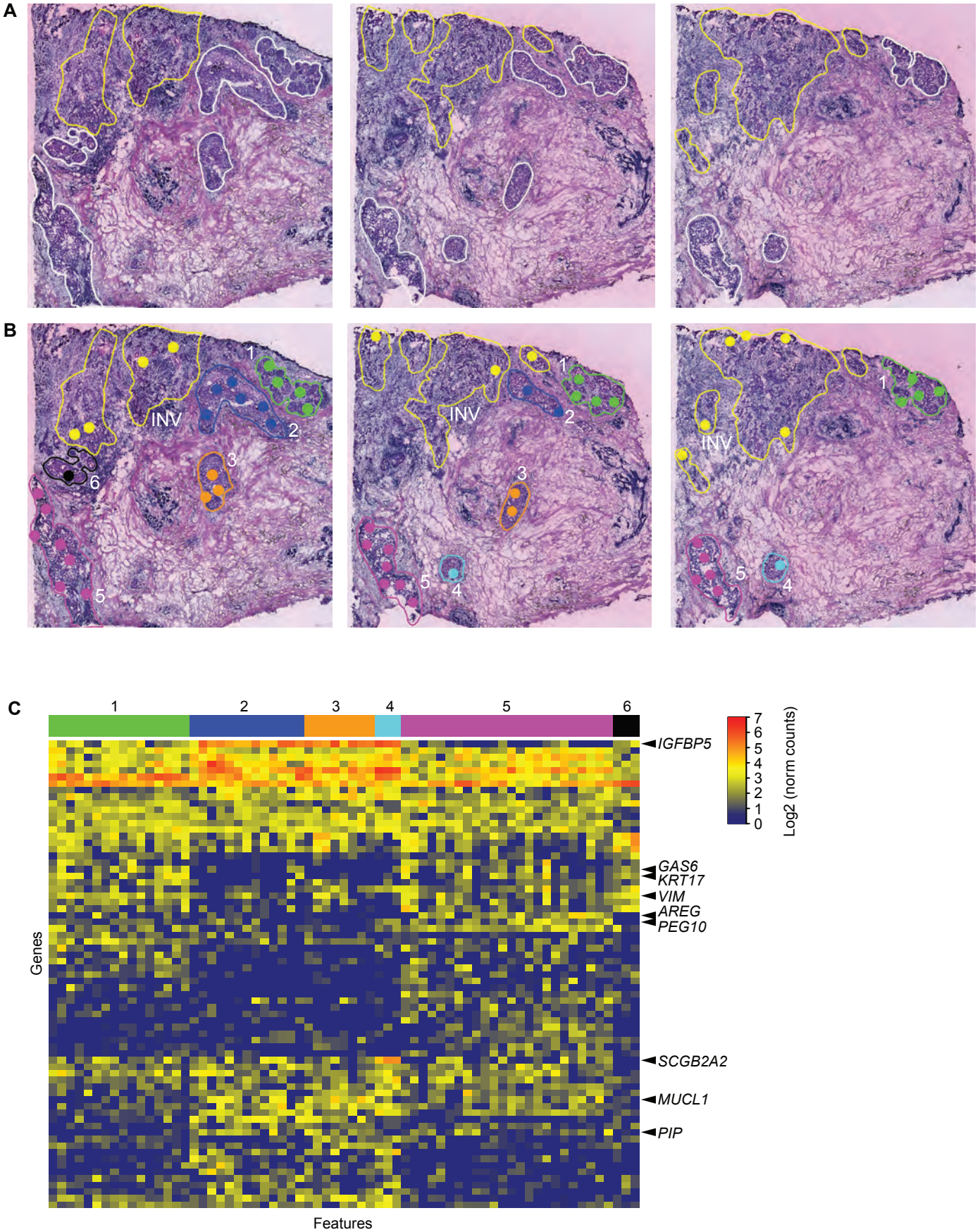

A
B
INV
1
2
3
4
5
6
C
1
2
3
4
5
6
IGFBP5
GAS6
KRT17
VIM
AREG
PEG10
SCGB2A2
MUCL1
PIP
Genes
Features
Log2 (norm counts)
7
6
5
4
3
2
1
0

Fig. S11. Adjacent sections from breast cancer biopsy

(A) Three more histological sections from the same breast cancer biopsy as shown in **Fig. 4C**, with invasive ductal cancer (INV) and six separate areas of ductal cancer in situ (1-6).

(B) Features, in the three sections shown in **(A)**, selected for Spatial Transcriptomics analysis. Only features in the INV area without or with minimal stromal infiltration were selected.

(C) Heatmap of differentially expressed genes between the six ductal cancer in situ areas shown in **(B)** and in **Fig. 4D**. The revealed expression patterns show a remarkable difference in genes expression profiles between areas of cancer in situ.

Table S1					
	mRNA and lncRNA	rRNA	mtRNA	Pseudogenes, repeats, artifacts	Unique transcripts after duplicate removal
On surface	23%	23%	24%	30%	9.6M (of 400M reads)
In solution	34%	6%	17%	43%	18 M (of 290M reads)

Table S1. Statistics from sequencing a library generated through cDNA synthesis from a tissue section on the surface of a spatially barcoded array and a library generated through cDNA synthesis of extracted RNA in solution.

Table S2		
	Average genes	Average transcripts
Granular cell layer	5390 +/- 1260	37400 +/- 14100
Mitral cell layer	6070 +/- 858	45400 +/- 16400
Outer plexiform layer	3640 +/- 648	17900 +/- 5850
Glomerular layer	5680 +/- 1030	38000 +/- 15800
Olfactory nerve layer	3390 +/- 763	14200 +/- 5310

Table S2. Average number of genes and unique transcripts captured from different cell layers of the adult mouse olfactory bulb through cDNA synthesis from a tissue section on the surface of a spatially barcoded array.

References and Notes

1. Z. Wang, M. Gerstein, M. Snyder, RNA-Seq: A revolutionary tool for transcriptomics. *Nat. Rev. Genet.* **10**, 57–63 (2009). Medline doi:10.1038/nrg2484

2. N. Crosetto, M. Bienko, A. van Oudenaarden, Spatially resolved transcriptomics and beyond. *Nat. Rev. Genet.* **16**, 57–66 (2015). Medline doi:10.1038/nrg3832

3. R. Satija, J. A. Farrell, D. Gennert, A. F. Schier, A. Regev, Spatial reconstruction of single-cell gene expression data. *Nat. Biotechnol.* **33**, 495–502 (2015). Medline doi:10.1038/nbt.3192

4. P. A. Combs, M. B. Eisen, Sequencing mRNA from cryo-sliced *Drosophila* embryos to determine genome-wide spatial patterns of gene expression. *PLOS ONE* **8**, e71820 (2013). Medline doi:10.1371/journal.pone.0071820

5. K. Achim, J. B. Pettit, L. R. Saraiva, D. Gavriouchkina, T. Larsson, D. Arendt, J. C. Marioni, High-throughput spatial mapping of single-cell RNA-seq data to tissue of origin. *Nat. Biotechnol.* **33**, 503–509 (2015). Medline doi:10.1038/nbt.3209

6. Materials and methods are available as supplementary materials on *Science* Online.

7. T. Hashimshony, F. Wagner, N. Sher, I. Yanai, CEL-Seq: Single-cell RNA-Seq by multiplexed linear amplification. *Cell Reports* **2**, 666–673 (2012). Medline doi:10.1016/j.celrep.2012.08.003

8. R. N. Van Gelder, M. E. von Zastrow, A. Yool, W. C. Dement, J. D. Barchas, J. H. Eberwine, Amplified RNA synthesized from limited quantities of heterogeneous cDNA. *Proc. Natl. Acad. Sci. U.S.A.* **87**, 1663–1667 (1990). Medline doi:10.1073/pnas.87.5.1663

9. R. Vassar, S. K. Chao, R. Sitcheran, J. M. Nuñez, L. B. Vosshall, R. Axel, Topographic organization of sensory projections to the olfactory bulb. *Cell* **79**, 981–991 (1994). Medline doi:10.1016/0092-8674(94)90029-9

10. K. D. Pruitt, G. R. Brown, S. M. Hiatt, F. Thibaud-Nissen, A. Astashyn, O. Ermolaeva, C. M. Farrell, J. Hart, M. J. Landrum, K. M. McGarvey, M. R. Murphy, N. A. O'Leary, S. Pujar, B. Rajput, S. H. Rangwala, L. D. Riddick, A. Shkeda, H. Sun, P. Tamez, R. E. Tully, C. Wallin, D. Webb, J. Weber, W. Wu, M. DiCuccio, P. Kitts, D. R. Maglott, T. D. Murphy, J. M. Ostell, RefSeq: An update on mammalian reference sequences. *Nucleic Acids Res.* **42** (D1), D756–D763 (2014). Medline doi:10.1093/nar/gkt1114

11. S. Zechel, P. Zajac, P. Lönnerberg, C. F. Ibáñez, S. Linnarsson, Topographical transcriptome mapping of the mouse medial ganglionic eminence by spatially resolved RNA-seq. *Genome Biol.* **15**, 486 (2014). Medline

12. D. Grün, A. van Oudenaarden, Design and analysis of single-cell sequencing experiments. *Cell* **163**, 799–810 (2015). Medline doi:10.1016/j.cell.2015.10.039

13. E. S. Lein, M. J. Hawrylycz, N. Ao, M. Ayres, A. Bensinger, A. Bernard, A. F. Boe, M. S. Boguski, K. S. Brockway, E. J. Byrnes, L. Chen, L. Chen, T.-M. Chen, M. C. Chin, J. Chong, B. E. Crook, A. Czaplinska, C. N. Dang, S. Datta, N. R. Dee, A. L. Desaki, T. Desta, E. Diep, T. A. Dolbeare, M. J. Donelan, H.-W. Dong, J. G. Dougherty, B. J. Duncan, A. J. Ebbert, G. Eichele, L. K. Estin, C. Faber, B. A. Facer, R. Fields, S. R.

Fischer, T. P. Fliss, C. Frensley, S. N. Gates, K. J. Glattfelder, K. R. Halverson, M. R. Hart, J. G. Hohmann, M. P. Howell, D. P. Jeung, R. A. Johnson, P. T. Karr, R. Kawal, J. M. Kidney, R. H. Knapik, C. L. Kuan, J. H. Lake, A. R. Laramee, K. D. Larsen, C. Lau, T. A. Lemon, A. J. Liang, Y. Liu, L. T. Luong, J. Michaels, J. J. Morgan, R. J. Morgan, M. T. Mortrud, N. F. Mosqueda, L. L. Ng, R. Ng, G. J. Orta, C. C. Overly, T. H. Pak, S. E. Parry, S. D. Pathak, O. C. Pearson, R. B. Puchalski, Z. L. Riley, H. R. Rockett, S. A. Rowland, J. J. Royall, M. J. Ruiz, N. R. Sarno, K. Schaffnit, N. V. Shapovalova, T. Sivisay, C. R. Slaughterbeck, S. C. Smith, K. A. Smith, B. I. Smith, A. J. Sodt, N. N. Stewart, K. R. Stumpf, S. M. Sunkin, M. Sutram, A. Tam, C. D. Teemer, C. Thaller, C. L. Thompson, L. R. Varnam, A. Visel, R. M. Whitlock, P. E. Wohnoutka, C. K. Wolkey, V. Y. Wong, M. Wood, M. B. Yaylaoglu, R. C. Young, B. L. Youngstrom, X. F. Yuan, B. Zhang, T. A. Zwingman, A. R. Jones, Genome-wide atlas of gene expression in the adult mouse brain. *Nature* **445**, 168–176 (2007). Medline doi:10.1038/nature05453

14. A. Mahfouz, M. van de Giessen, L. van der Maaten, S. Huisman, M. Reinders, M. J. Hawrylycz, B. P. Lelieveldt, Visualizing the spatial gene expression organization in the brain through non-linear similarity embeddings. *Methods* **73**, 79–89 (2015). Medline

15. L. J. P. van der Maaten, G. E. Hinton, Visualizing data using t-SNE. *J. Mach. Learn. Res.* **9**, 2579–2605 (2008).

16. M. Kittaneh, A. J. Montero, S. Glück, Molecular profiling for breast cancer: a comprehensive review. *Biomarkers Cancer* **5**, 61–70 (2013).

17. C. Gjerdrum, C. Tiron, T. Høiby, I. Stefansson, H. Haugen, T. Sandal, K. Collett, S. Li, E. McCormack, B. T. Gjertsen, D. R. Micklem, L. A. Akslen, C. Glackin, J. B. Lorens, Axl is an essential epithelial-to-mesenchymal transition-induced regulator of breast cancer metastasis and patient survival. *Proc. Natl. Acad. Sci. U.S.A.* **107**, 1124–1129 (2010). Medline doi:10.1073/pnas.0909333107

18. S. Lundin, H. Stranneheim, E. Pettersson, D. Klevebring, J. Lundeberg, Increased throughput by parallelization of library preparation for massive sequencing. *PLOS ONE* **5**, e10029 (2010). Medline

19. N. Schaeren-Wiemers, A. Gerfin-Moser, A single protocol to detect transcripts of various types and expression levels in neural tissue and cultured cells: In situ hybridization using digoxigenin-labelled cRNA probes. *Histochemistry* **100**, 431–440 (1993). Medline doi:10.1007/BF00267823

20. A. Lyubimova, S. Itzkovitz, J. P. Junker, Z. P. Fan, X. Wu, A. van Oudenaarden, Single-molecule mRNA detection and counting in mammalian tissue. *Nat. Protoc.* **8**, 1743–1758 (2013). Medline doi:10.1038/nprot.2013.109

21. B. Langmead, S. L. Salzberg, Fast gapped-read alignment with Bowtie 2. *Nat. Methods* **9**, 357–359 (2012). Medline doi:10.1038/nmeth.1923

22. S. Anders, P. T. Pyl, W. Huber, HTSeq—a Python framework to work with high-throughput sequencing data. *Bioinformatics* **31**, 166–169 (2015). Medline doi:10.1093/bioinformatics/btu638

23. P. I. Costea, J. Lundeberg, P. Akan, TagGD: Fast and accurate software for DNA Tag generation and demultiplexing. *PLOS ONE* **8**, e57521 (2013). Medline doi:10.1371/journal.pone.0057521

24. M. I. Love, W. Huber, S. Anders, Moderated estimation of fold change and dispersion for RNA-seq data with DESeq2. *Genome Biol.* **15**, 550 (2014). Medline doi:10.1186/s13059-014-0550-8

25. L. Wang, S. Wang, W. Li, RSeQC: Quality control of RNA-seq experiments. *Bioinformatics* **28**, 2184–2185 (2012). Medline doi:10.1093/bioinformatics/bts356